JOURNAL OF GEOPHYSICAL RESEARCH, VOL. 100, NO. D8, PAGES 16,765–16,791, AUGUST 20, 1995

# Intercomparison of UV/visible spectrometers for measurements of stratospheric $NO_2$ for the Network for the Detection of Stratospheric Change

David Hofmann,[1] Paolo Bonasoni,[2] Martine De Maziere,[3] Franco Evangelisti,[2] Giorgio Giovanelli,[2] Aaron Goldman,[4] Florence Goutail,[5] Jerald Harder,[6] Roger Jakoubek,[6] Paul Johnston,[7] Jim Kerr,[8] W. Andrew Matthews,[7] Tom McElroy,[8] Richard McKenzie,[7] George Mount,[6] Ulrich Platt,[9] Jean-Pierre Pommereau,[5] Alain Sarkissian,[5] Paul Simon,[3] Susan Solomon,[6] Jochen Stutz,[9] Alan Thomas,[7] Michel Van Roozendael,[3] and Edmund Wu[8]

**Abstract.** During the period May 12-23, 1992, seven groups from seven countries met in Lauder, New Zealand, to intercompare their remote sensing instruments for the measurement of atmospheric column $NO_2$ from the surface. The purpose of the intercomparison was to determine the degree of intercomparability and to qualify instruments for use in the Network for the Detection of Stratospheric Change (NDSC). Three of the instruments which took part in the intercomparison are slated for deployment at primary NDSC sites. All instruments were successful in obtaining slant column $NO_2$ amounts at sunrise and sunset on most of the 12 days of the intercomparison. The group as a whole was able to make measurements of the 90° solar zenith angle slant path $NO_2$ column amount that agreed to about ±10% most of the time; however, the sensitivity of the individual measurements varied considerably. Part of the sensitivity problem for these measurements is the result of instrumentation, and part is related to the data analysis algorithms used. All groups learned a great deal from the intercomparison and improved their results considerably as a result of this exercise.

## 1. Introduction

The Network for the Detection of Stratospheric Change (NDSC) was formed in 1986 as an international organization to develop a ground-based measuring network specifically designed to provide the earliest possible detection of changes in the composition and structure of the stratosphere and the means to understand the causes of those changes. It is also intended to provide extremely valuable scientific returns in the near term by siting a number of sophisticated instruments together in a small number of observatories around the globe. To that end, a number of instruments have been built to measure stratospheric species. Among the prime instrument set is designated instrumentation to measure nitrogen dioxide ($NO_2$).

$NO_2$ plays an important role in the photochemistry of stratospheric ozone [*Crutzen*, 1970; *Johnston*, 1971; *Johnston and Podolske*, 1978] and is the nitrogen species directly responsible for the catalytic control of ozone, which, along with NO, plays a vital role in coupling the $NO_x$ and $ClO_x$ families. Large ozone and $NO_2$ depletions have been measured in the polar regions [e.g., *McKenzie and Johnston*, 1984; *Mount et al.*; 1987, *Sanders et al.*; 1989, *Wahner et al.*, 1989; *Johnston et al.*, 1992; *Goutail et al.*, 1992, 1994a,b; *Kondo et al.*, 1994; *Perner et al.*, 1994; *Pommereau and Piquard*, 1994). The ozone depletions have been attributed to elevated levels of chlorine which postulate high levels of ClO inside the polar vortex. High values of ClO cannot exist if $NO_2$ is high because the $NO_2$ would be converted to $ClONO_2$ via the reaction

$$ClO + NO_2 + M \rightarrow ClONO_2 + M \quad (1)$$

Low springtime concentrations of $NO_2$ allow buildup of chlorine-destroying ClO. Thus the measurement of $NO_2$ is of critical importance to understanding the chemistry of the perturbed stratosphere.

The instruments that measure $NO_2$ in the stratosphere follow the basic design of *Brewer et al.* [1973] and *Noxon* [1975]. The spectrum of the zenith sky at various solar zenith angles is measured, and from knowledge of the changing air mass it is possible to deduce a slant column abundance of $NO_2$ (and other molecules). These spectrographs operate in the

[1]NOAA Climate Monitoring and Diagnostics Laboratory, Boulder, Colorado.
[2]Institute Fisbat, CNR, Bologna, Italy.
[3]Belgian Institute for Space Aeronomy, Brussels.
[4]Department of Physics, University of Denver, Denver, Colorado.
[5]Service d'Aeronomie, CNRS, Verrières, France.
[6]NOAA Aeronomy Laboratory, Boulder, Colorado.
[7]National Institute of Water and Atmospheric Research, Lauder, New Zealand.
[8]Atmospheric Environment Service, Toronto, Ontario, Canada.
[9]Institute for Environmental Physics, University of Heidelberg, Heidelberg, Germany.



Paper number 95JD00620.
0148-0227/95/95JD-00620$05.00

ultraviolet and visible portion of the spectrum and typically utilize array detectors for simultaneous observation of a large spectral region (tens of nanometers). Since the early 1980s, a number of instruments have been developed to measure $NO_2$ and other species, and since the NDSC program is interested in selecting those instruments that meet a high standard of measurement ability, it was decided to hold an official and blind intercomparison of the abilities of the current instruments.

Prior to this instrument intercomparison, an informal comparison of data analysis algorithms (S. Solomon and P. Johnston, unpublished manuscript, 1990) was held in an attempt to understand the different algorithms developed for data analysis by different groups. This would be an essential step to complete, since inevitably the comparison of the instruments would involve the data analysis techniques. This exercise (described in more detail in section 3) demonstrated that analyzing the same spectra using algorithms developed by different groups did not produce the same results unless considerable effort was made to make the analysis parameters, such as cross sections and spectrum alignment method, the same. This data analysis intercomparison was a formal one with an independent referee (A. Goldman, University of Denver) and involved sending each participant sets of real instrument data and the matching molecular cross-section data. The workshop ended with the agreement to have a second-phase data analysis intercomparison using synthetic spectra. One reason for using synthetic spectra is that the inputs are known, and so absolute accuracy can be evaluated. Controlling the inputs also enabled the addition of random noise to see how algorithms handled it. This exchange has occurred, and the results are briefly described in section 3.

After completion of the data analysis intercomparison, the instrument intercomparison was held May 12-23, 1992. The site selected was Lauder, New Zealand, where clean air (to avoid problems with tropospheric pollution) is prevalent and where a substantial number of credible $NO_2$ measurements have been made over the past 10 years. This formal and blind intercomparison was attended by seven formal and one informal participants with an independent referee (D. Hofmann, NOAA Climate Monitoring and Diagnostics Laboratory, Boulder, Colorado). Discussions by correspondence were held with all participants to formulate the intercomparison rules and the referee's role. The referee's primary role was to ensure the strict formality of the intercomparison, to collect and monitor the results as they were collected in the field, to insure frequent and proper use of the $NO_2$ calibration standards by instruments in the field, and to prepare and distribute the results. No participant saw any other participant's data prior to release of the data by the referee at a workshop 4 months after the intercomparison was complete. No one was allowed to change their data after the formal required submission date 6 weeks after close of field operations.

This paper describes the measurement technique for determining $NO_2$, the campaign in New Zealand, the individual instruments, and the results.

## 2. Stratospheric $NO_2$ Twilight Zenith Measurement Technique

Stratospheric $NO_2$ has been measured using the twilight zenith technique by a number of workers since the early 1970s. *Brewer et al.* [1973] first reported results, and their work was followed by that of others who studied the spatial and temporal variability of stratospheric $NO_2$ and improved significantly the instrumentation so that sensitivity was much increased [*Noxon*, 1975, 1979; *Noxon et. al.*, 1979; *Harrison*, 1979; *Syed and Harrison*, 1981; *McKenzie and Johnston*, 1982, 1983; *Ridley et al.*, 1984; *Shibasaki et al.*, 1986; *Mount et al.*, 1987; *Pommereau and Goutail*, 1988a,b; *Goutail et al.*, 1994a,b; *Kondo et al.*, 1994; *Perner and Piquard*, 1994; *Pommereau and Piquard*, 1994]. A ground-based spectrometer views the zenith sky at twilight to measure in the visible or near-UV spectral regions of scattered sunlight, the absorptions by $NO_2$ and other trace gases. The absorption amounts depend on solar zenith angle (SZA) and the altitude of the absorbers because of the changing light scattering, and therefore fractional contribution to the spectrum, with altitude. Because sunlight passes nearly tangentially through the atmosphere before being scattered down to the spectrometer, these absorptions are enhanced relative to those seen in light that might have passed vertically through the same atmosphere. Interpretation of the measured absorptions both at a fixed SZA (typically 90°) and over a range of SZAs can be used to calculate $NO_2$ vertical column amounts and estimate $NO_2$ altitude profiles. For recent work with such scattering models, see *Solomon et al.*, [1987], *McKenzie et al.*, [1991], *Perliski and Solomon*, [1992, 1993], and *Brion et al.*, [1994]. A measured $NO_2$ result is usually expressed as a "slant" column amount in molecules per square centimeter although no physical column is implied. The actual vertical column $NO_2$ is usually calculated from the slant column by dividing by an air mass factor (AMF), also called an enhancement factor (EF), derived using a scattering model. For an SZA of 90°, a wavelength of 450 nm, and an absorber altitude between 20 and 25 km, the AMF is approximately 20 [*Perliski and Solomon*, 1992]. By comparison, for a midday SZA of 35°, the AMF is approximately 1.2 and can be directly computed from sec (SZA).

Various instruments have been used to measure zenith sky spectra. These include flat field spectrographs using array detectors [e.g.; *Mount et al.*, 1992], scanning monochromators using photomultiplier detectors [*McKenzie and Johnston*, 1982], and instruments that sample at discrete wavelengths [*Kerr*, 1989]. All workers use a data analysis process to calculate slant column $NO_2$ from the observed spectral absorption. Absorptions by any other major absorbers in the wavelength region used, such as $O_3$ and $H_2O$, are also often seen in the spectra and are also analyzed.

To remove the large (typically 20 to 40% of mean intensity) solar Fraunhofer features present in the spectra, the analysis uses the log of the ratio of a twilight to a midday spectrum. For stratospheric absorbers, the AMF at twilight is usually much larger than the AMF at midday, and so the use of this ratio technique almost completely removes the unwanted solar Fraunhofer absorptions while retaining the stratospheric absorptions. Most analyses use minimum least squares fitting of the cross sections of the expected absorbers to the ratio spectrum. Shift and stretch of the two spectra forming the ratio is usually included as part of the fitting optimization, making it a nonlinear process. Subtle effects such as Ring effect [*Grainger and Ring*, 1962] must also be dealt with to reduce the error margin.

Both the instrument and analysis can introduce errors, of which few are truly random. The residual spectra from the fitting process usually show systematic features indicating that bias errors are likely. This makes the understanding of errors

very important for the long-term measurement of stratospheric change. In the following we outline the major known sources of error.

### 2.1. Instrumental Error

Spectrometers and spectrographs deviate from the ideal in a variety of ways, some of which can influence the derived results. Grating imperfections, other grating orders, scattered light, and reentrant light can introduce stray spectral features that may correlate with the fitted cross sections. Optical aberrations may change the instrument function from the expected slit function, and these changes may vary across an array detector, making the precise fitting of literature-reported cross sections difficult. Stray light may introduce a wavelength-dependent offset in spectra. Diffraction gratings invariably introduce polarization-dependent artifacts in spectra and since the zenith skylight is always partly polarized, such artifacts depend on spectrometer orientation with respect to the Sun, solar zenith angle, aerosol loading, and sky cloudiness. Detectors can introduce both near-constant offset and structured features in the spectra. Diode array detectors introduce many problems, including etaloning modulation of the spectrum from passivation layers, scattering from reflection off the passivation layer, and leakage (dark) current subtraction problems, which introduce peculiar waves into the spectra at the sub-0.1% level and are dependent on detector temperature [*Mount et al.*, 1992]. Etaloning in the array detector alone can result in a 20% modulation of the spectrum, and the phase of the modulation can change with time if precautions are not taken.

### 2.2. Analysis

The analysis method used plays an important role in interpretation of the data and the ultimate noise level achieved by the instrument. It can reduce errors both random and systematic in nature by, for example, accommodating instrument-introduced artifacts in the spectra, or it can introduce errors that are not inherent in the spectra. Clearly, analysis cannot be separated from the spectrometer and its data sampling; they are intimately intertwined. A useful way to describe the sampling frequency (in wavelength) is to give the number of samples per full width half maximum (FWHM) for the instrument function. The instruments intercompared ranged from approximately 1.5 to more than 10 samples per FWHM. The NDSC data analysis intercomparison showed that higher sampled data produced lower errors [*Goldman*, 1991, 1992]. Noise in the ratio spectrum is produced by the interpolation used to shift and stretch the twilight and midday spectra so that they are properly wavelength aligned with each other before the ratio spectrum is formed. Incorrect alignment causes "leakage" of the dominant solar Fraunhofer features. Interpolation noise is lower when more frequent sampling is used. The need for alignment arises from the mechanical changes in the spectrometer or spectrograph due to temperature variations and aging. It is interesting to note that some systems do this alignment well enough that their residual spectra are a factor of a thousand or more smaller than the solar Fraunhofer absorptions.

Artifacts in the ratio spectrum produced by the grating polarization characteristics can be approximately modeled to reduce biases in $NO_2$ results. One technique is to derive a cross section that mimics the artifacts from measurements using a polarizer. Use of such a cross section also helps to reduce residuals so other residual errors can be identified.

An important requirement for obtaining low residuals is that all known spectral shapes be fitted to the log ratio spectrum in the analysis. This would normally include slope and constant, to accommodate atmospheric transmission and spectrometer gain differences between the midday and twilight measurements, the Rayleigh scattering function (see below), Ring effect (see below), any spectrometer polarization artifact shape, and all known significant absorbers in the wavelength region used. In the 400- to 490-nm region, absorbers include $NO_2$, $O_3$, $H_2O$ (near 442 nm), and $O_4$ (near 447 and 478 nm).

### 2.3. Scattering Physics

Because the spectrometer measures scattered light, the spectral features introduced by scattering should be considered. Rayleigh fourth order curvature can be well modeled, as can Mie (essentially a slope for short wavelength intervals), but the spectrum of the Ring effect is much more difficult. It can, however, be measured (as suggested by A. Schmeltekopf [*Solomon et al.*, 1987]) and used as a cross section to approximately fit for the effect. Because the Ring effect is arguably primarily due to rotational Raman scattering [*Solomon et al.*, 1987], it is unpolarized. This weak unpolarized light combined with the partially polarized Rayleigh-scattered light produces a spectrum that depends on the spectrometer and sky polarization characteristics, making it more difficult to model in most cases.

### 2.4. $NO_2$ Cross Sections

Most published $NO_2$ measurements have used $NO_2$ cross sections measured at room temperature rather than at the stratospheric temperatures required. In the stratosphere, temperature-induced shape changes introduce residuals in the analysis (S. Solomon, private communication, 1993), since the stratosphere is not isothermal and the differential cross section magnitude is larger by between 10 and 20% [*Leroy et al.*, 1987]. For a critical review on the question of measuring the cross section of $NO_2$ at low temperatures and a summary of existing work, see *Roscoe and Hind* [1993]. Figure 1 shows a residual with $NO_2$ cross-section temperature structure remaining.

Systematic features in the residual spectra (for instruments where residual spectra are available) provide the experimenter with evidence of possible systematic errors. The importance of these can often be estimated by tests such as varying the analysis wavelength interval to determine upper error limits and determine if the same abundance is derived for a given molecule using different wavelength intervals. More insidious are the effects of constant or near-constant offsets in the measured spectra, such as caused by stray light or detector offsets and nonlinearities. The signature of these can almost disappear in the ratio spectrum, so the experimenter may see low residuals but the retrieved results can be in error. For example, if the mean intensity of a measured twilight and midday spectrum is 1.0 and an offset of 0.1 of the mean intensity is added to both, then a derived result will be approximately 10% lower than true. If this offset is added to only one of the two spectra forming the ratio, then a clear signature of the solar Fraunhofer will result, enabling identification of the problem. The only sure way to determine that offsets are not producing errors is for the experimenter to design against them.

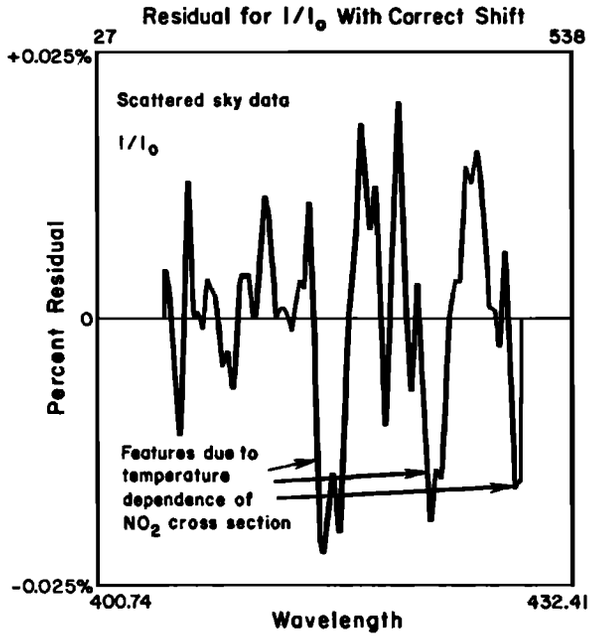


**Figure 1.** Percent residual absorption in the 400- to 432-nm spectral region after removal of linear and fourth-order terms and room temperature ozone and nitrogen dioxide. The spectral ratio was formed from spectra at 90° and 83° solar zenith angle. The instrument was the NOAA spectrometer.

## 3. UV/Visible Data Analysis Intercomparisons

Prior to and during the NDSC UV/visible intercomparisons, two rounds of evaluating data analysis techniques were conducted. In the first round, the results of which were presented at the meeting held in Boulder, Colorado, on July 23-25, 1991 [*Goldman*, 1991], the following groups participated: Max-Planck-Institut für Chemie (MPIC), Germany (group A); ITA, Spain (group B); FISBAT, Italy (group C); Department of Scientific and Industrial Research (DSIR), (now National Institute of Water and Atmospheric Research or NIWA), New Zealand (group E); National Oceanic and Atmospheric Administration (NOAA), United States (group F); and Centre National de la Recherche Scientifique (CNRS), France (group G). Three sets of observed spectroscopic data, from measured full days of zenith sky spectra, along with the relevant absorption cross sections were provided by three of the groups: DSIR, CNRS, and NOAA. In additition, several sets of synthetic spectra for analysis were generated with undisclosed gas amounts.

The objectives were (1) case 1 tests, to develop a standard method to validate intercomparisons of instruments and analysis, (2) case 2 tests, for individual groups' "best" analysis, by extending modeling of the atmosphere (with the Ring effect) and instrumentation, and (3) synthetic spectra tests, for the study of sampling and noise problems. Observed spectra selected for the intercomparisons were obtained at different locations, but with common wavelength regions. Other considerations for the selection of observed spectra included resolution, scan time and coaddition of spectra, consistency of the scans, signal to noise ratio for high and low Sun, diurnal variations, spectral sampling, interpolation, and filtering.

Descriptions of the data analysis methods by the individual groups are provided in the 1991 report. For the data analysis it was important that the reference solar spectra came from the same instrument and that the reference $NO_2$ and $O_3$ cross sections were adjusted to each specific instrument function, requiring shifting, stretching, and interpolating each spectrum, which was achieved by various approaches by the different groups (e.g., minimization of residuals, maximization of correlation). In the spectral fitting, temperature- and pressure-independent slant path gas column amounts were derived.

The spectra were wavelength calibrated, ratioed with the reference spectrum, detrended, and differenced to reduce nonessential correlations for fitting with the corresponding differential cross sections. Both single-parameter iterations and multiparameter fits were used in linear and nonlinear spectral least squares. Examination of the residuals versus signal to noise ratio allows validation of unaccounted spectral features (mostly from solar lines and unknown trace gases). Error estimates for the column abundances were sought, both random and systematic.

For the intercomparisons of case 1 tests, three experimental data sets referred to as NOAA1, DSIR1, and CNRS1, were analyzed by four groups. While the residuals were close to the signal to noise ratio in all analyses, in regions of known spectral absorption, various degrees of agreement were found. In general, it was found that the $NO_2$ tests were more compatible than the $O_3$ tests. The best agreement between the groups was obtained in the analysis of the NOAA1 data. These data had the most coadding, the lowest photon noise, the highest spectral sampling, and the least interference of $H_2O$. In the analysis of the DSIR1 data, the agreement between the groups was quite close. The worst agreement occurred in the analysis of the CNRS1 data. It appeared that CNRS's own analysis method was best for that data. Some of the best results are shown in Figure 2 for $NO_2$ analysis of the NOAA1 data. In case 2 tests, with the DSIR2, NOAA2, and CNRS2 data sets, the differences between the groups were similar to those found in case 1 tests. These intercomparisons indicated that case 1

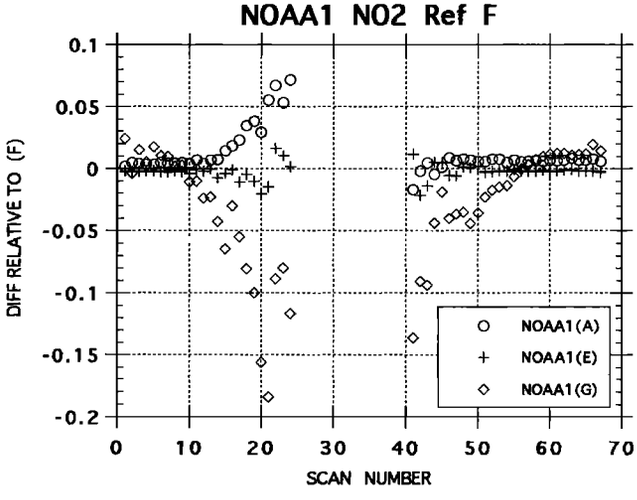


**Figure 2.** Differences, relative to group F, as a function of the spectrum scan number, of the slant path column amount analysis of the NOAA1 (F) $NO_2$ observed data set. The graph shows the three groups that were in closest agreement. The range of scans, left to right, covers A.M. and P.M. with zenith angles of 72° to 97° [*Goldman*, 1991].

standard tests should be limited to 75°-93° to avoid low or highly scattered signals, respectively. The divergence between the groups was particularly significant at high Sun angles. Several analyses, however, showed improved sensitivity over others for both low and high Sun angles.

In the synthetic spectra tests, it was found that in cases where no $NO_2$ or $O_3$ were included in the simulated spectra, some analyses retrieved $NO_2$ and $O_3$ abundances, while most analyses found these undefined. An order of magnitude improvement was achieved in the residuals in the case of increased sampling, and all groups verified that $NO_2$ and $O_3$ were unretrievable.

It became clear that it is essential to increase the data sampling and to specify in detail the interpolation and filtering methods used for the solar reference spectrum, the atmospheric absorption spectra, and cross sections. It was recognized that improved laboratory $NO_2$ and $O_3$ cross sections at high resolution with both temperature and pressure dependence are needed. Analysis of the algorithms revealed several incompatibilities between the methods used, some of which require a wider wavelength range for the retrievals than that provided by the data. The importance of a correct wavelength scaling, with both shift and stretch, is evident for all the algorithms.

The second round of data analysis and algorithms intercomparison was dedicated to the retrievals of $NO_2$, $O_3$, and OClO from synthetic spectra. These spectra, prepared by P.V. Johnston (group E), included several subsets with various combinations of $NO_2$, $O_3$, OClO, Rayleigh (i.e., fourth order), Ring, wavelength shift and stretch, and noise over the wavelength range 405-475 nm. Combinations were made at both fine and coarse sampling.

The results of the intercomparisons were presented at Boulder, Colorado, on October 13-15, 1992, during the instrument intercomparison results [*Goldman*, 1992]. The following groups participated: MPIC, Germany (A); ITA, Spain (B); FISBAT, Italy (C); DSIR, New Zealand (E); NOAA, United States (F); CNRS, France (G); Cambridge University, England (H); NASA Langley Research Center (K); and Belgian Institute for Space Aeronomy (BISA), Belgium (M). It was found that best agreement between the groups was obtained in cases of no shifts, no stretch and fine sampling. Worst agreement occurred when the synthetic spectra included large shifts, large stretch, and coarse sampling. The differences between the group's results, in order of priority, were driven by wavelength shift and stretch, sampling, Rayleigh, and Ring.

The best agreement was obtained for $NO_2$ and then for $O_3$. The retrievals of OClO were often marginal. It was encouraging that several groups reached agreement within ±3% for almost all cases. Some of the best results are shown in Figures 3 and 4. The groups' total range of disagreement was much larger, up to 20%. It was recognized that additional algorithm developments are needed.

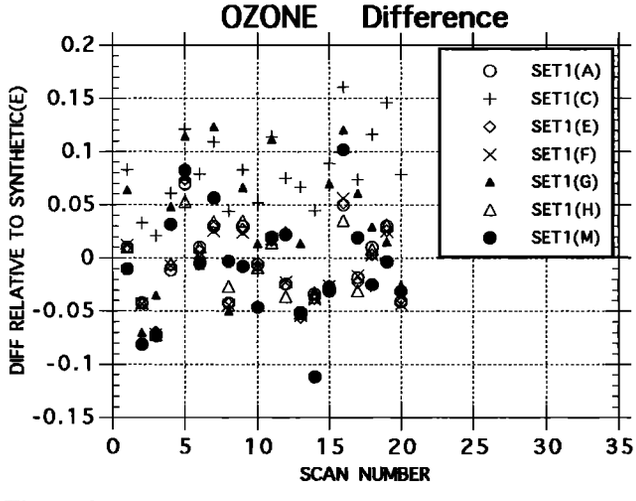


**Figure 3.** Relative differences, as a function of the spectrum scan number, of the column amount analysis of the synthetic $O_3$ spectra REF (E). The graph shows the seven groups that were in closest agreement [*Goldman*, 1992].

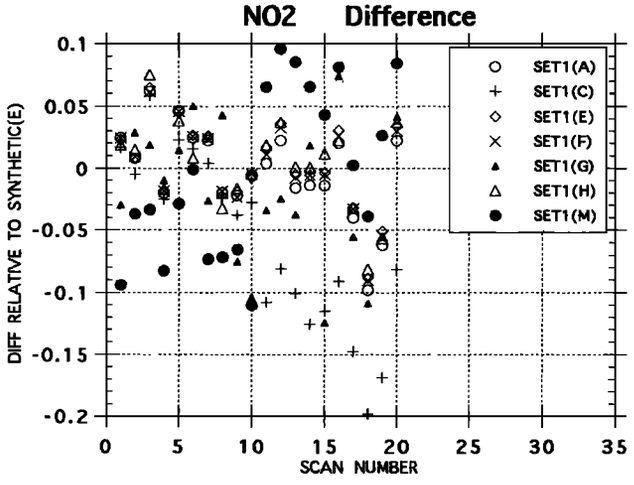


**Figure 4.** Same as Figure 3 but for the synthetic $NO_2$ spectra REF (E).

## 4. Instrument Descriptions

All of the instruments that participated in the intercomparison were spectrometers operating in the ultraviolet and visible regions of the spectrum. Figure 5 shows the spectral resolution of each instrument using the 435.8-nm Hg line from a calibration lamp. Most instruments had a nominal 1-nm full width at half maximum response. Group C's was somewhat smaller while those of groups H and I were

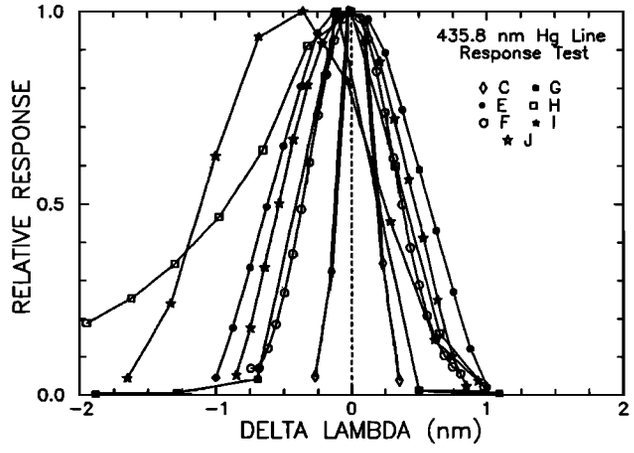


**Figure 5.** Response of the seven spectrometers to the 435.8-nm mercury line.

somewhat larger. Most used some type of array detector, but one used a photomultiplier tube. Some scanned the spectral region and some had no moving parts. Some used a large spectral interval for evaluation, while others used a part (or parts) of the spectrum for analysis for $NO_2$. The types of spectrometers varied from simple Ebert-Fastie systems to Rowland circle and crossed Czerny-Turner types, and most were single systems, although one was a double spectrometer to reduce scattered light. Most of the systems used a telescope to limit the field of view; fields of view varied from a fraction of a degree (NOAA) to over 30° (CNRS). Some of the systems are designed to operate outdoors, while others require installation in a building. Analysis algorithms were substantially different, and most had been evaluated as part of the data intercomparison discussed earlier. Thus substantially different types of spectral instrumentation were used. Brief descriptions of each participating instrument follow.

### 4.1. New Zealand Group

The NIWA-Lauder instrument used in the intercomparison is an *f*/5 Czerny-Turner spectrometer (Instruments S A Inc., model HR 320) with a set of entrance mirrors that split the view of the zenith sky into two components orientated so that each view is normal to the other. This reduces the sensitivity to polarization effects. The spectrometer has a 320-mm focal length, uses spherical mirrors, and a 68-mm-square plane holographic grating to ensure that stray light is less than 0.2%. The slits are 1 x 12 mm, which produces a 1.3-nm FWHM slit function. Sampling every 0.125 nm in scan wavelength results in a sampling frequency of approximately 10 samples per FWHM. The detector is an EMI 9804A photomultiplier tube, and the gain is adjusted by over 5 orders of magnitude by varying the dynode chain voltage from 400 to 1400 V. For this campaign, wavelength was scanned from 432 to 487 nm by rotating the grating using a lead screw plus sine bar mechanism driven by a stepper motor. The manufacturerís mechanism was modified in house to improve scan repeatability and life expectancy. The preprogrammed twilight measurements are centered at an integer SZA value and consist of 10 scans, each taking 18 s. The whole system, spectrometer, electronics, and computer, is sufficiently portable that it can, after being deployed inside a building, be calibrated and operating in a few hours. The computer program does a full nonlinear fit of known absorbers and prints preliminary results after each measurement.

### 4.2. Italian Group

The basic configuration of the FISBAT-Consilio Nazionale delle Riceriche (CNR) spectrometer comprises (1) a 150-cm *f*/5 Cassegrainian telescope which focuses the incoming light onto a 100 μm x 2.0 mm entrance slit; (2) a Jobin-Yvon spectrometer with holographic spherical diffraction grating of 1200 grooves/mm, with a spectral dispersion of 2.4 nm/mm at 300 nm, and spectral analysis at 50-nm steps through a stepper motor; (3) a Hamamatsu multichannel detector that integrates a 512 metal-oxide semiconductor (MOS) diode array detector with 50 μm x 2.5 mm pixels; and (4) a band-pass filter wheel to reduce stray light in the spectrograph. The readout time of the entire detector is 40 ms. The most suitable integration time for each spectral reading is selected automatically and ranges from several seconds at noon to a maximum value of 240 s at twilight. A Peltier-element cooling system and a temperature controller keep the detector's temperature at -25°±0.1°C. At this temperature the dark current signal is not negligible for long integration times and hence is always measured and subtracted from the overall detected signal. The maximum time period for each spectral reading was about 6 min. Given the instrument's 0.5-nm overall optical resolution and the diffraction grating's optical dispersion of about 0.12 nm/diode, approximately four detector diodes constitutes one resolution element. An Hg lamp, mounted within a central hole in the telescope's secondary mirror, is automatically used periodically to check the position of the diffraction grating. The system took automatic and unattended spectral readings as per predefined measurement cycles and was located outside for the entire period of the intercomparison.

### 4.3. French Group

The CNRS SAOZ is a broadband, 300- to 600-nm, diode array instrument which views the zenith sky, with a total field of view of 30°, through a quartz window and a baffle and *f*/3 aperture of the concave holographic grating. Baffles are also mounted inside the spectrometer for reducing internal stray light. The entrance slit corresponds to the size of a single pixel (25 μm x 2.5 mm) of the detector. The spectral sampling is one pixel per full width at half maximum. The detector is a low dark current NMOS Hamamatsu 512-diode array. There is no cooling. A 12-bit analog to digital conversion gives a noise of 1 count out of 4096. The spectrum is read out in 10 ms and the integration time, which is adjusted automatically, ranges from 0.1 s at noon to a maximum of 60 s at twilight (dark current saturation at 100 s for a detector temperature of 20°C). The spectral analysis, performed in real time, consists of ratioing the actual spectrum to an $I_o$ spectrum after wavelength alignment by shift and stretch. Rayleigh and Mie scattering are removed by broadband filtering. The amount of absorbants ($NO_2$, $O_3$, $O_4$, and $H_2O$) are calculated and then removed in a sequential and iterative linear least squares fit process. The Ring contribution is removed by using an empirical "cross section" consisting of the narrow-band structures of the differential $I_o$ spectrum. $NO_2$ is measured between 405 and 498 nm on a total of more than 20 bands, and $O_3$ is measured between 450 and 588 nm. The instrument was fully operational throughout the intercomparison period.

### 4.4. Belgian Group

The Belgian instrument used a grating spectrograph coupled to a 1024-element diode array detector. The spectrograph was a commercial f/3.7 crossed Czerny-Turner from Oriel, Inc. (type Multispec) of 125 mm focal length with a flat focal field adequate for use with diode arrays as long as 25 mm. The entrance slit was 100 μm wide and 3 mm high. With a 600 groove/mm
ruled grating, the resultant resolution was 1.35 nm FWHM. The full spectral range extended from 280 to 600 nm, with a sampling ratio of about four points per resolution element (FWHM). The detector from Princeton Instruments was equipped with a 1024-pixel EG&G Reticon scientific silicon photodiode array protected by a quartz window. The array was cooled down to -45°C by a two-stage Peltier cooler by flowing methanol at the regulated temperature of -8°C through the heat removal circuit. Mounted outdoors inside a watertight

container kept at constant temperature, the spectrograph looked directly toward the zenith through a hemispherical dome of fused silica. The full angle field of view was 15°. The data were analyzed using an iterative least squares algorithm [*Pommereau and Goutail*, 1988a,b], incorporating absorption cross sections of known atmospheric absorbers in the wavelength range from 405 to 452 nm ($NO_2$, $O_3$, $O_4$) as well as a pseudo cross section for the Ring effect generated by high-pass filtering of the reference spectrum. The absorption cross sections were taken from the literature and convolved with the measured instrument function. In order to compensate for the small-wavelength drifts of the spectrometer, the algorithm allowed the alignment of the twilight spectrum with the reference spectrum by appropriate shifting.

### 4.5. German Group

The instrument developed at the University of Heidelberg observes zenith scattered light by a quartz lens of 50 mm diameter and a focal length of 100 mm. The light is focused on the circular end of a depolarizing quartz fiber bundle of 3-m length. The opposite end of the bundle is slit shaped (2.5 mm x 60 μm) and feeds a *f*/2.2 spectrograph with a flat field holographic grating (710 grooves/mm and *f*=100 mm). The spectrograph is thermally stabilized at 28±0.3°C. The light is detected by a windowless EG&G 1024-element random access photodiode array, cooled to -35°C by a three-stage Peltier cascade cooler mounted on a fan-cooled heat sink. The diode array detector housing is filled with argon. Digital conversion of the signals is accomplished by a 16-bit analog to digital converter (ADC) with approximately 1000 photoelectrons per count. Integration time varies from a few seconds at noon to a maximum value of 300 s at high zenith angles. A section of the spectrum, 436 nm to 452 nm (50 pixels), was analyzed. Spectra were corrected for electronic offset, dark current, and etalon and diode structures. The spectra were divided by a polynomial of degree 5 to reduce remaining etalon structures. The twilight spectrum was shifted and fitted to the $I_0$, to minimize $c^2$. In the last step a $NO_2$ reference spectrum was fitted, together with a ring spectrum and an additive polynomial of degree 3. The instrument was operating during the entire campaign except for the morning of day 143, when a power failure occured. Problems due to a fast changing etalon structure were reported to the referee at the third day of the campaign. It was decided, nevertheless, to continue with the participation in the intercomparison campaign, knowing that the etalon problem would increase the measurement error (see section 7.5).

### 4.6. Canadian Group

The Atmospheric Environment Service (AES) Brewer instrument is a modified Ebert spectrograph which has multiple exit slits and a lens near the entrance slit to correct for coma and astigmatism. The spectrograph produces a spectrum at the exit slit plane that has a near-linear dispersion of about 1 nm/mm. A set of five slits are precision-milled into a blackened stainless steel sheet which is mounted on the focal plane. The relative positions and widths of these slits are very precisely controlled by fabricating them using laser machining. In the ozone-measuring mode the spectrum is adjusted so that the five exit slits are positioned at appropriate points in the ozone and solar spectra. The operational wavelengths for ozone and sulfur dioxide measurements are 306.3, 310.1, 313.5, 316.0, and 320.0 nm. $NO_2$ is measured by the Brewer spectrophotometer by observing the zenith sky at the five wavelengths 431.42, 437.34, 442.82, 448.10, and 453.22 nm [*Kerr*, 1989]. These wavelengths are not specifically optimized for $NO_2$ measurement on an individual basis. They are chosen so that the slit mask, which has been optimized for ozone measurement in the diffraction grating third order, can be used to select the $NO_2$ measurement wavelengths as well. The $NO_2$ measurements are made using the grating in the second order.

The light transmitted at each of the wavelengths is recombined by a Fabry lens located just behind the spectrometer focal plane. It produces a reduced image of the diffraction grating on the 10-mm-diameter photocathode of an EMI, Inc. 9789Q photomultiplier tube. The various slits (wavelengths) are sampled sequentially in time by selectively opening and closing them using a motor-driven mask mounted in front of the slits. Since the slits remain stationary and are only opened and closed by the mask, the wavelength sampled by each slit remains very stable. The data from the Brewer are collected by the same IBM-PC-compatible computer that controls the automatic sequencing of observations. The Brewer instrument is fully weatherproofed and was mounted out of doors during the entire intercomparison period. The method used to analyze the Brewer $NO_2$ data has been reported elsewhere [*Kerr*, 1989].

### 4.7. U.S. Group

The NOAA instrument views the zenith sky with a field of view 0.1°x1.0° using an off-axis parabolic telescope. The telescope feeds an entrance slit of dimension 250 μm x 3.0 mm where light enters a double crossed Czerny-Turner spectrograph of 3/8 m focal length (each side) and *f*/7 speed. The spectrograph feeds a 1024-element diode array detector with 25 μm x 2.5 mm pixels which correspond to 0.06 nm per pixel in dispersion. Total spectral coverage centered on 430 nm was about 60 nm. Spectral sampling was 10 pixels per full width at half maximum on a spectral feature. We have found this oversampling of the spectral profile critical to getting low-residual spectra. The detector has a data range of $2^{16}$, and each data number corresponds to about 900 electrons. Noise is about 3 data numbers (1 sigma standard deviation) and is mostly random. There is a very small amount of systematic noise from the clocking pulses. The spectrum is read out in 65 ms at the end of each integration. Typical integration times range from a fraction of a second at noon to a maximum allowed time of 300 s at twilight. (300 s is about 5° of SZA change at latitude 45°). A double system was chosen to reduce the effects of scattered light, and a crossed system was chosen to allow excellent baffling, not possible in a standard Czerny-Turner system. The data are analyzed using a nonlinear least squares algorithm which incorporates the following: known molecular spectra in the region near 425 nm (e.g., $NO_2$, $O_3$, OClO), mathematically represented functions such as Rayleigh and Mie scattering slopes, Ring effect as measured with a polarizer, shift and stretch of the two spectra being ratioed, and artifacts such as polarization. Typical residual spectra at 90° solar zenith angle run a few hundredths of a percent peak-to-peak. The instrument worked for the entire period of the intercomparison and required only minor tuneup on arrival at the Lauder station.

**Table 1.** Intercomparison Participants

| Group Affiliation | Code Letter |
|---|---|
| Istituto Fisbat, CNR, Bologna, Italy | C |
| National Institute of Water and Atmospheric Research, Lauder, New Zealand | E |
| NOAA Aeronomy Laboratory, Boulder, Colorado | F |
| CNRS Service d'Aeronomie, Verrieres, France | G |
| Institute for Environmental Physics, University of Heidelberg, Heidelberg, Germany | H |
| Belgian Institute for Space Aeronomy, Brussels, Belgium | I |
| Atmospheric Environment Service, Toronto, Ontario, Canada | J |

## 5. The Lauder Intercomparison Campaign

The $NO_2$ intercomparison was conducted at the DSIR (now NIWA) Atmospheric Research Facility at Lauder, New Zealand (45°S), during the period May 12-23, 1992 (days 133-144). Table 1 lists the institutions that took part in the intercomparison and gives the code letter used for each group in this report. All of the instruments were located within 500 m of each other at the observing site and the center of their field of view observed the zenith sky and were nominally coincident.

### 5.1. Solar-Meteorological Conditions

The viewing conditions during the intercomparison period are summarized in Table 2 and Figure 6. Table 2 presents subjective observations of the daily cloud cover during the intercomparison campaign. The data presented are daily estimates of cloud cover in the morning, at midday and in the evening, and the daily ozone column where available. The fractional values represent the portion of the sky covered by clouds. Solar illumination can be inferred from Figure 6, which shows the relative detector count rate of the group F instrument averaged over the wavelength range 400-460 nm. This instruments has a 0.1° x 1.0° field of view; an instrument with a different field of view would give somewhat different results. Data in this figure are arbitrarily normalized to the count rate of the spectrum obtained at local (clock) noon on day 138, when the zenith sky was clear, which was used as the standard $I_o$ for the intercomparison. The histogram which appears on this figure shows the relative count rate of the spectrum that occurred at minimum solar zenith angle, which was used for the daily $I_o$. It can be seen in this figure that days 133, 139, 143, and 144 were relatively clear days and had a daily $I_o$ that was comparable in count rate to that at1200 local time on day 138, the standard $I_o$ value. The other days had higher count rates due to multiple scattering caused by the overlying cloud cover.

### 5.2. Standard Cell Calibrations and Data Normalization

The use of standard gas cells is a common method to check the operation of UV-visible spectrometers. Thus a set of standard $NO_2$ cells, to be passed among the observing groups taking part in the intercomparison, was considered necessary in order to be sure each instrument was working properly and to provide a standard and known check on cross sections used by each group in its analysis. It is difficult to prepare standards which do not change with time owing to leaks, contamination,

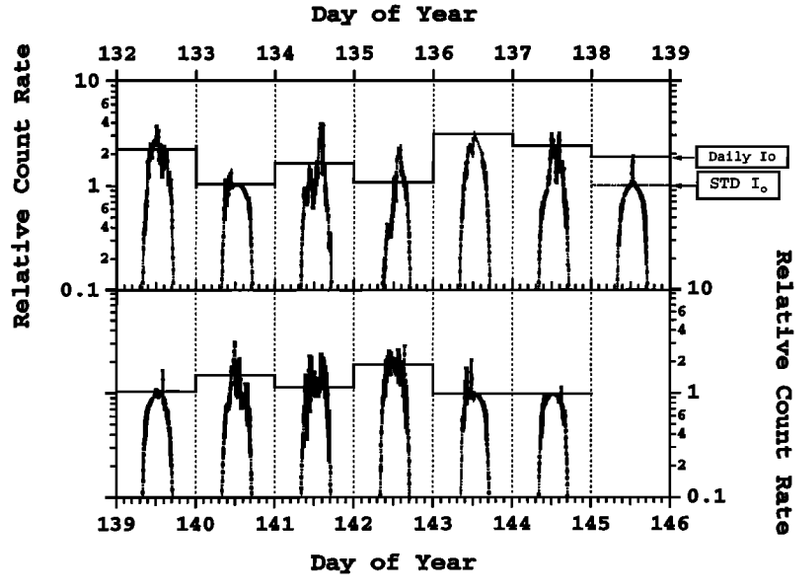


**Figure 6.** Solar intensity as measured at 400-460 nm with the group F spectrometer for each day of the intercomparison. The values of daily $I_o$, chosen by this group at local noon, are indicated by the solid horizontal lines. The value of the standard $I_o$, chosen by this group at clock noon on day 138, is indicated by the dashed horizontal line. Cloudiness is indicated by enhancements above the clear sky envelope (e.g., day 144) in scattered radiation.

**Table 2.** Cloud Cover and Ozone Data

| Day | A.M. Cloud | Midday Cloud | P.M. Cloud | Dobson Ozone, DU | SAOZ Ozone, DU |
|---|---|---|---|---|---|
| 133 | mainly clear | mainly clear | clear | 288 | 301 |
| 134 | thin | variable | 7/8 | ---- | 285 |
| 135 | 8/8,thin | variable | 7/8 | ---- | 279 |
| 136 | 8/8 | variable | 8/8 | ---- | 281 |
| 137 | mainly clear | variable | 7/8 | 284 | 281 |
| 138 | thin | clear@12:00 | clear | 289 | 288 |
| 139 | clear | mainly clear | mainly clear | 283 | 283 |
| 140 | mainly clear | variable | mainly clear | 310 | 295 |
| 141 | 6/8, variable | partly clear | 6/8, variable | ---- | 308 |
| 142 | 6/8, night snow | variable | clear patches | ---- | 279 |
| 143 | 7/8 | clear | 5/8 | 278 | 289 |
| 144 | clear | clear | 7/8 | 302 | 288 |

etc.; however, time did not allow the preparation of standards and subsequent long-term monitoring of their stability prior to the intercomparison. Shortly before the intercomparison referee's deployment to New Zealand, A. Ravishankara, of the NOAA Aeronomy Laboratory in Boulder, prepared three $NO_2$ standards and one blank cell. The three standard cells each had different $NO_2$ concentrations, with values in the expected annual 90° SZA $NO_2$ slant column range at Lauder, New Zealand (A.M., 3-8 x $10^{16}$ cm-2, P.M., 4-12 x $10^{16}$ cm-2). The actual values were known only to the manufacturer and the referee and are given in the footnote to Table 4 (nominally 4, 8, and 17 x $10^{16}$ cm-2).

Prior to the campaign, it was decided that since each group would be using different cross sections, analysis techniques, etc., the best way to intercompare data in the field was to choose one of the standard cells as a calibration cell, conduct a calibration on the first day, compare the derived value with the known value, and provide each group with a correction factor which was to be applied by the participants to their data sets throughout the campaign. In this way, each group was responsible for normalizing their own data, thus simplifying the referee's task and preventing the possible unfortunate occurrence of mathematical errors by the referee. This would also allow the referee to determine early on that no group had serious problems which were going unnoticed. Although this procedure was generally successful, continued calibrations during the campaign indicated that some groups were obtaining inconsistent data. As will be elaborated on later, in the most serious case, this was caused by a temperature effect on the amount of $NO_2$ in the cell and the fact that some instruments were outside in an uncontrolled temperature environment. Fortunately, this was discovered early enough in the campaign so that the required test data could be gathered to reduce the impact on the intercomparison.

On the first official day of the campaign, day 133, standard cell 2 (~8 x $10^{16}$ cm-2), chosen as the calibration cell, and the blank cell with identical windows were measured three times by each group (except group J, for which this calibration was conducted on day 134), and an average correction factor was determined. Table 3 shows the correction factors (multiplicative) for each group initially and the final values used for the intercomparison. The initial correction factors ranged from 0.96 to 1.61. The 1.61 initial value (group H) was the result of erroneous cross sections which could not be corrected in the field, and it was agreed that it would be adjusted after the intercomparison. All group H data given here are with the new cross section subsequently applied, which gave a correction factor of 1.06. The 1.32 initial value (group G) turned out to be a result of the temperature effect alluded to earlier and was reduced prior to completion of the intercomparison. The other smaller changes in correction factors were the result of reanalysis after the 6 days of calibrations with cell 2, spread out over the campaign, were completed. All three standard cells were measured on 5 days during the campaign. The results, without corrections, are given in Table 4 and in Figure 7 along with the actual (7%) values. Figure 8 shows all calibrations with cell 2 for all groups before and after the final correction factors were applied. Although the improvement is not great, because home group (E) was chosen to be the group which the referee would use to compare all others with, and since they were the only group which indicated more $NO_2$ in the cells than was actually present, the correction turned out to be significant for the intercomparison and indicates that different groups were normalizing to different published values of $NO_2$ absolute cross section.

Figure 8 indicates that group G observed a gradual increase in the amount of $NO_2$ in calibration cell 2 over the campaign. Figure 9 shows the standard cell results of the Boulder group (F) during the campaign and 5 months later with the same spectrometer, under the same temperature conditions at Fritz Peak, Colorado. The three cells appear to have been stable to about 10% (less in the case of cell 3) over this period. Thus cell drift was not a problem during the campaign. Temperatures during the calibrations varied from a few degrees Celsius for outside instruments on the coldest days to room temperature for the inside instruments. The cells were kept in insulated dark containers until placed over the entrance windows of the instruments. Thus outside instruments would be making

**Table 3.** Correction Factors Determined From Standard Cell 2

| Group | Initial Correction Factor | Final Correction Factor |
|---|---|---|
| C | 1.06 | 1.03 |
| E | 0.96 | 0.96 |
| F | 1.08 | 1.08 |
| G | 1.32 | 1.06 |
| H | 1.61 | 1.06* |
| I | 1.13 | 1.05 |
| J | 1.07 | 1.07 |

*Determined after the intercomparison from new cross sections.

**Table 4.** $NO_2$ Cell Calibrations

| DAY | C1 | C2 | C3 | E1 | E2 | E3 | F1 | F2 | F3 | G1 | G2 | G3 | H1 | H2 | H3 | I1 | I2 | I3 | J1 | J2 | J3 |
|---|---|---|---|---|---|---|---|---|---|---|---|---|---|---|---|---|---|---|---|---|---|
| 133* | - | 7.59 | - | - | 8.37 | - | - | 7.48 | - | - | 6.11 | - | - | 7.50 | - | - | 7.16 | - | - | - | - |
| 134 | 3.43 | 7.81 | 17.7 | 4.32 | 8.62 | 18.3 | 3.90 | 7.61 | 16.3 | 3.21 | 6.53 | 15.9 | 3.85 | 8.13 | 16.8 | 3.88 | 7.87 | 17.2 | 3.46 | 7.56 | 16.9 |
| 136 | 3.82 | 8.37 | 18.3 | 4.22 | 8.61 | 18.3 | 3.86 | 7.43 | 15.9 | 3.83 | 6.92 | 15.3 | 3.74 | 7.55 | 15.6 | 3.30 | 7.52 | 16.9 | 3.84 | 7.51 | 16.3 |
| 139 | 3.44 | 7.84 | 18.0 | 4.10 | 8.54 | 18.2 | 3.78 | 7.43 | 16.0 | 3.59 | 7.32 | 15.8 | 3.74 | 7.63 | 16.8 | 3.38 | 7.41 | 16.7 | 2.46 | 6.51 | 15.5 |
| 141 | 4.12 | 7.79 | 17.5 | - | - | - | 3.83 | 7.45 | 16.0 | 3.75 | 7.26 | 15.8 | 3.80 | 7.78 | 16.4 | 3.90 | 7.60 | 16.7 | 3.26 | 6.94 | 15.0 |
| 143 | 3.76 | 7.54 | 18.1 | 4.40 | 8.44 | 18.3 | 3.88 | 7.53 | 16.1 | 3.89 | 7.59 | 15.7 | 3.65 | 8.08 | 16.7 | 3.76 | 7.75 | 17.0 | 3.38 | 7.37 | 16.0 |

Units are $10^{16}$ molecules $cm^{-2}$. Laboratory values (±7%) were as follows: cell 1, 3.96 x $10^{16}$ $cm^{-2}$, cell thickness 1 cm; cell 2, 8.06 x $10^{16}$ $cm^{-2}$, cell thickness 1 cm; and cell 3, 16.92 x $10^{16}$ $cm^{-2}$, cell thickness 2 cm.
*Average of three measurements on Cell 2

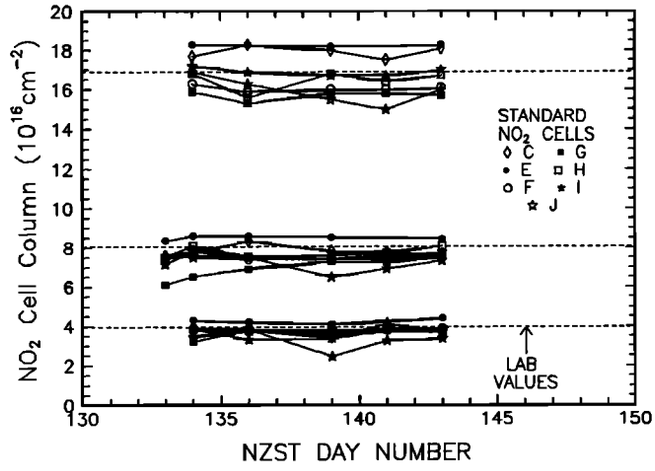


**Figure 7.** Results of standard $NO_2$ cell calibrations on 6 days of the intercomparison. The dashed lines represent values measured in the laboratory prior to the campaign.

measurements on cells which were changing temperature during the first few minutes. Because measurement procedures were not as well defined in the initial measurements, the first group G calibration with cell 2 was not done rapidly, and the cell temperature reached ambient (8°-10°C) before data were taken. Subsequently, the procedure was accelerated, and data could be taken while the cell was still warmer than ambient. This indicated that as the cell cooled down, the amount of inferred $NO_2$ decreased by 10-20%. An experiment was conducted in which the cell was placed at ambient, cold temperature into the warm group F spectrometer which was capable of rapid (25 s) measurements. Both the group G cooldown on 2 days, and the group F warmup test results are given in Figure 10, with the latter indicating about a 15% increase in $NO_2$ concentration in the cell over the 8°C to 22°C difference in outside and inside temperature.

The increase in $NO_2$ with temperature is due to dissociation of the dimer $N_2O_4$, which forms in the cell, as the cell warms up. The applicable equilibrium rate constant is given by 5.9 x $10^{-29}$ exp(6600/T) $cm^3$ $molecule^{-1}$ [*Jet Propulsion Laboratory*, 1992]. Cell 2 had an $NO_2$ molecular concentration of about 8 x $10^{16}$ $cm^{-3}$ (the cell was 1 cm thick), so that at 8°C the dimer to $NO_2$ concentration fraction would be about 7.5% while at 22°C it would be about 2.5%. Thus a 5% decrease in the dimer for a temperature change from 8°C to 22°C would result in an $NO_2$ increase of 10%, consistent with what was observed in the group F spectrometer.

## 6. Results

All groups made measurements during the sunrise and sunset periods (denoted hereinafter by A.M. and P.M.); some measured throughout the day. Clocks were synchronized, and New Zealand Standard Time was used as the independent variable for recording measurements. Each group also converted their times to SZA in the data files submitted to the referee each day. A daily measurement was conducted by each group at local noon (minimum SZA or about 1230 local time), $I_o$, which was used in the analysis. One day was chosen for a "standard" $I_o$, which was also used in the analysis. This day happened to be day 138; however, clock noon was chosen for the measurement time, as the zenith was cloud-free at this time

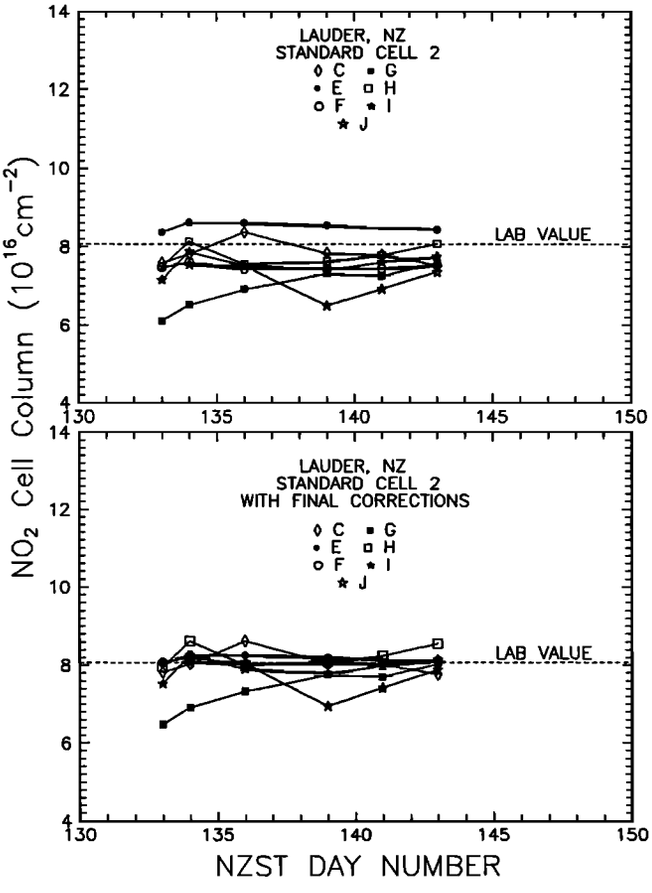


**Figure 8.** Results of calibrations with standard cell 2 (top) before and (bottom) after final correction factors were applied to the data. The dashed lines represent the value measured in the laboratory prior to the campaign.

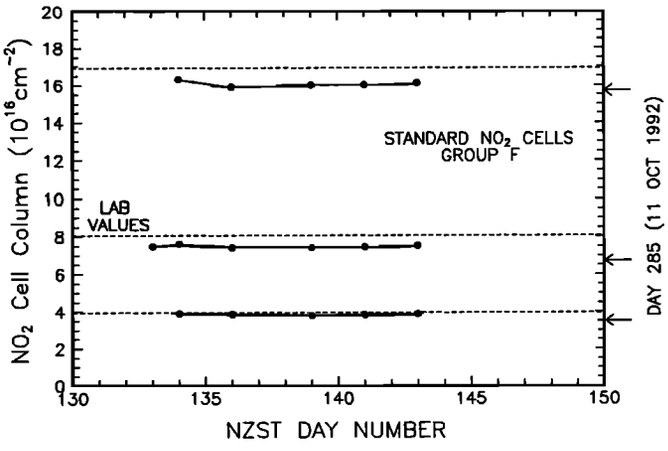


**Figure 9.** Group F measurements of the standard $NO_2$ cells during the intercomparison and 5 months later with the same spectrometer. The dashed lines represent values measured in the laboratory prior to the campaign.

with clouds moving in at local noon (see solar intensity data in Figure 6).

The technique of taking data was not standardized, and each group used their normal procedure. Thus the individual data-taking interval methods varied among groups, with some taking short measurements with longer intervening times and some integrating over relatively long periods with essentially no intervening time. For example, group G measured for about 2 min with about 5 min between measurements, while group F measured continuously, integrating data for 5 min with only seconds between measurements. Group C varied its total measurement time, increasing as solar zenith angle increased. The host group (E) was programmed to automatically take 5-min measurements centered on integer values of SZA. In the following, all data will be presented with final $NO_2$ cell correction factors applied.

### 6.1. $NO_2$ Slant Column Values

Figure 11 is an example of P.M. measurements by all groups for 2 days. Here $NO_2$ slant column values are displayed versus time of measurement with a bar connecting data points indicating the integration period. The 2 days chosen also indicate the general range of agreement of measurements among groups, with day 136 showing relatively good agreement and day 144 unusually poor. This was somewhat surprising, since day 144 was the most cloud-free during the campaign, while day 136 was cloudy several hours before and after noon. Day 144 was also the last day of the campaign. The P.M. measurements, with their higher signal to noise, generally produced better agreement than the A.M. measurements.

Each group also provided daily A.M. and P.M. 90° SZA $NO_2$ slant column values for daily and standard $I_0$, which they obtained from their data through interpolation (except for group E, whose data were already in integer SZA values). Figure 12 shows these data versus time during the campaign for each group. Most groups show similar features in their data. $NO_2$ column values appear to have increased initially, then leveled off for several days, took a dip around day 140, then increased and decreased again by day 144. The fact that there were variations in $NO_2$ column values as large as 30% was fortunate, as it aids in evaluating instrument sensitivity. All groups appear to agree on the $NO_2$ column values for 90° SZA to 20% or so, although in the case of group J, the shape of the $NO_2$ versus time curve does not agree well with the other

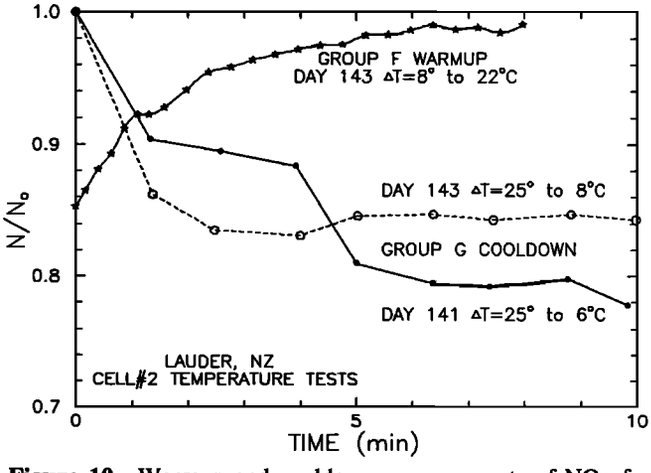


**Figure 10.** Warmup and cooldown measurements of $NO_2$ for standard cell 2, indicating dissociation and formation of the $N_2O_4$ dimer with the group F and G spectrometers, respectively.

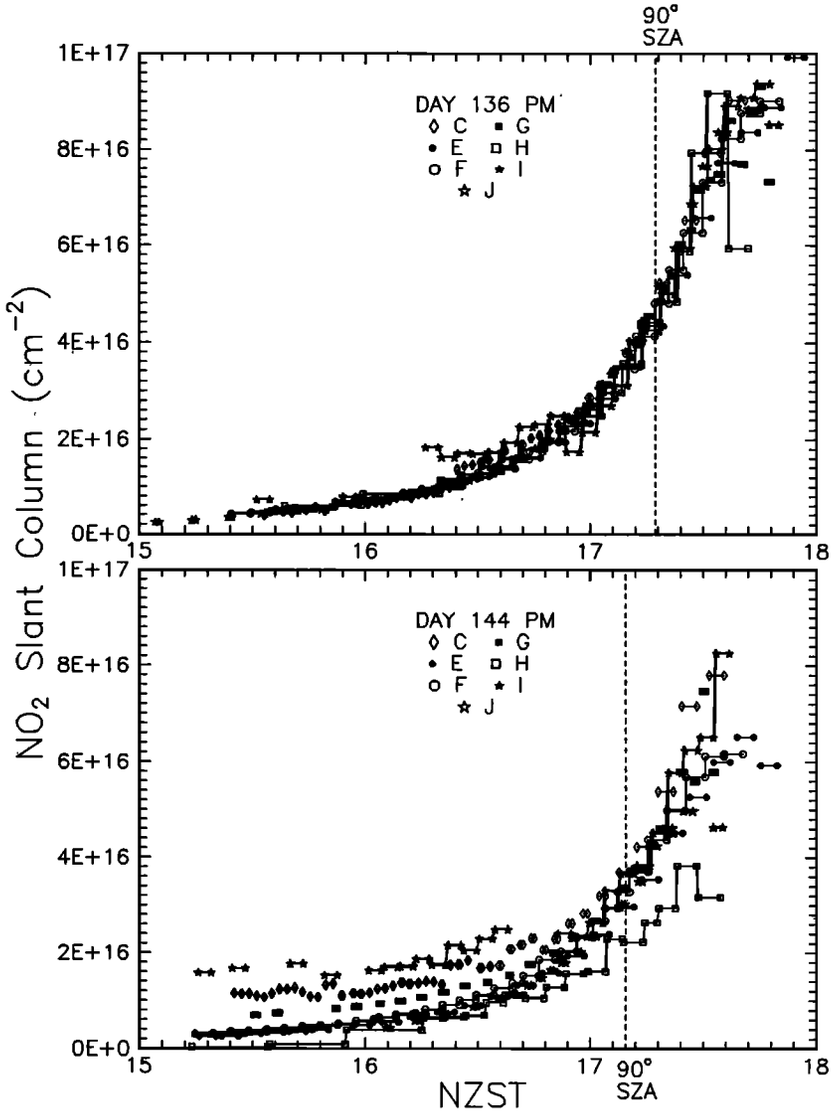


**Figure 11.** Examples of $NO_2$ slant column versus local time evening measurements by all groups on 2 days, representing a "good" (top) day and a "bad" (bottom) day . Horizontal bars represent integration times. The time of 90° solar zenith angle is indicated by the vertical dashed line.

groups. Groups E and F appear to obtain essentially the same values for both daily and standard $I_o$, with groups G and I also obtaining reasonable agreement. The remaining groups show substantial differences for different $I_o$ values, especially group C, which indicates values about 20% higher than other groups when standard $I_o$ was used.

Data in Figure 12 indicate that $NO_2$ column values were relatively constant for 5 consecutive days (134 through 138). Figures 13 and 14 show the A.M. and P.M. $NO_2$ slant columns for daily and standard $I_o$, respectively, for these days. Values at small solar zenith angles (high Sun) give a good measure of the signal to noise capability of the instrument, since the air mass factors are changing very slowly and so slant column $NO_2$ is also changing only slowly. Values at large solar zenith angles (low Sun) give a good measure of the sensitivity of the instrument, since light levels are quite low under these conditions. Groups E and F show relatively constant values for these days, even for small SZA when signal to noise is low with only a slight degradation at the small-SZA end when standard $I_o$ is used. Groups G and I, while giving consistent values for these days near 90° SZA, give considerably poorer results at smaller SZA when the signal is small. Group G appears to give slightly more consistent results when standard $I_o$ is used. The remaining groups give relatively poorer results, regardless of $I_o$, especially at small SZA. All groups appear to give their best values near 90° SZA, which is understandable since the light level is still fairly high while the absorption has increased by about a factor of 10 from that at 65° SZA (local noon).

### 6.2. Comparisons With the Host Group

Figures 15 and 16 show comparisons, using daily $I_o$, of each group with the host group (E) for day 138, a relatively good day in terms of agreement and day 144, a relatively poor day. On the latter day, even groups E and F, which gave consistent results throughout most of the intercomparison, indicated differences of the order of 10% in the P.M. data. Groups C and

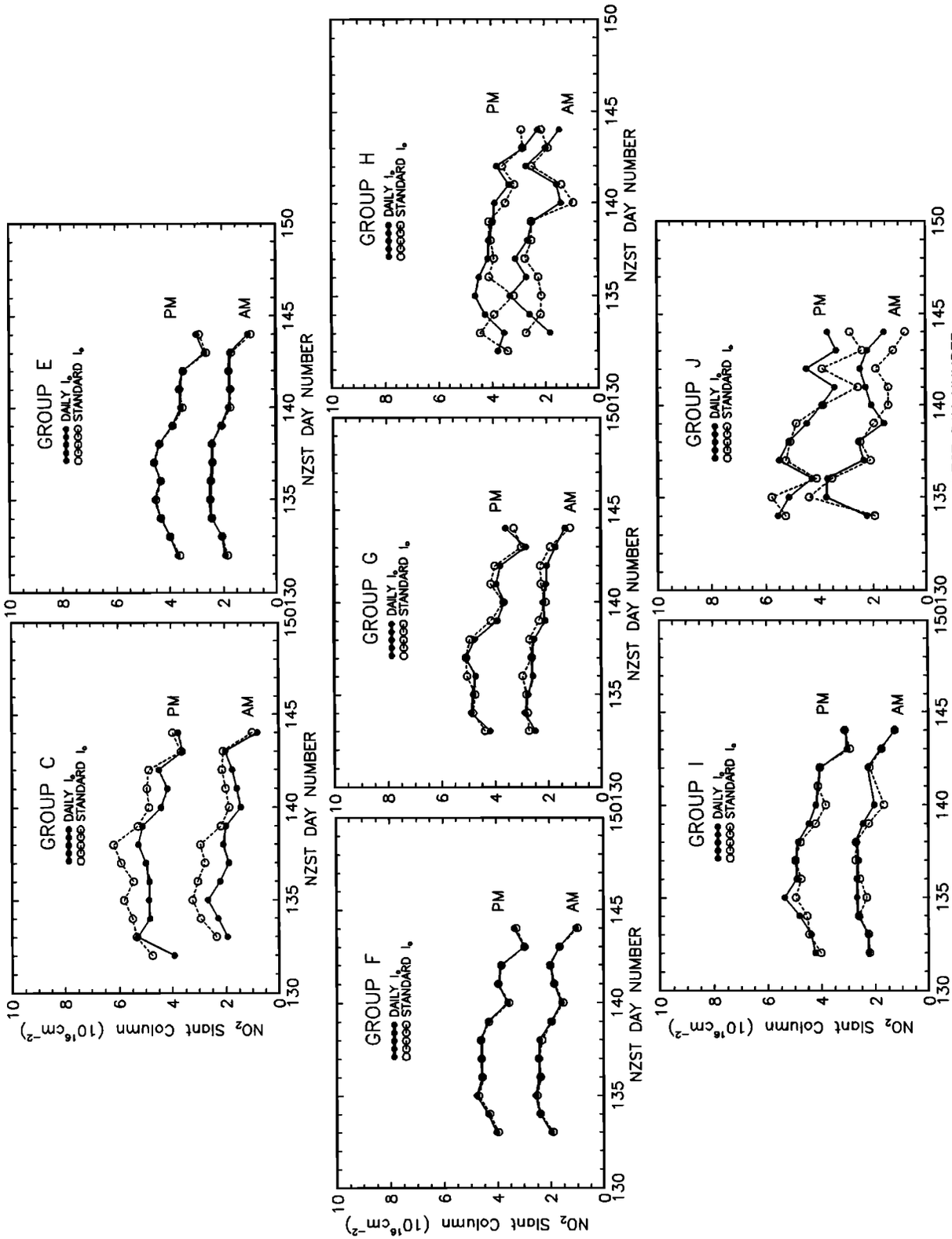


**Figure 12.** Morning and evening daily values of 90° solar zenith angle slant column $NO_2$ measured by each group for $I_o$ measured on each day (solid circles) and for a single (standard) $I_o$ (open circles).

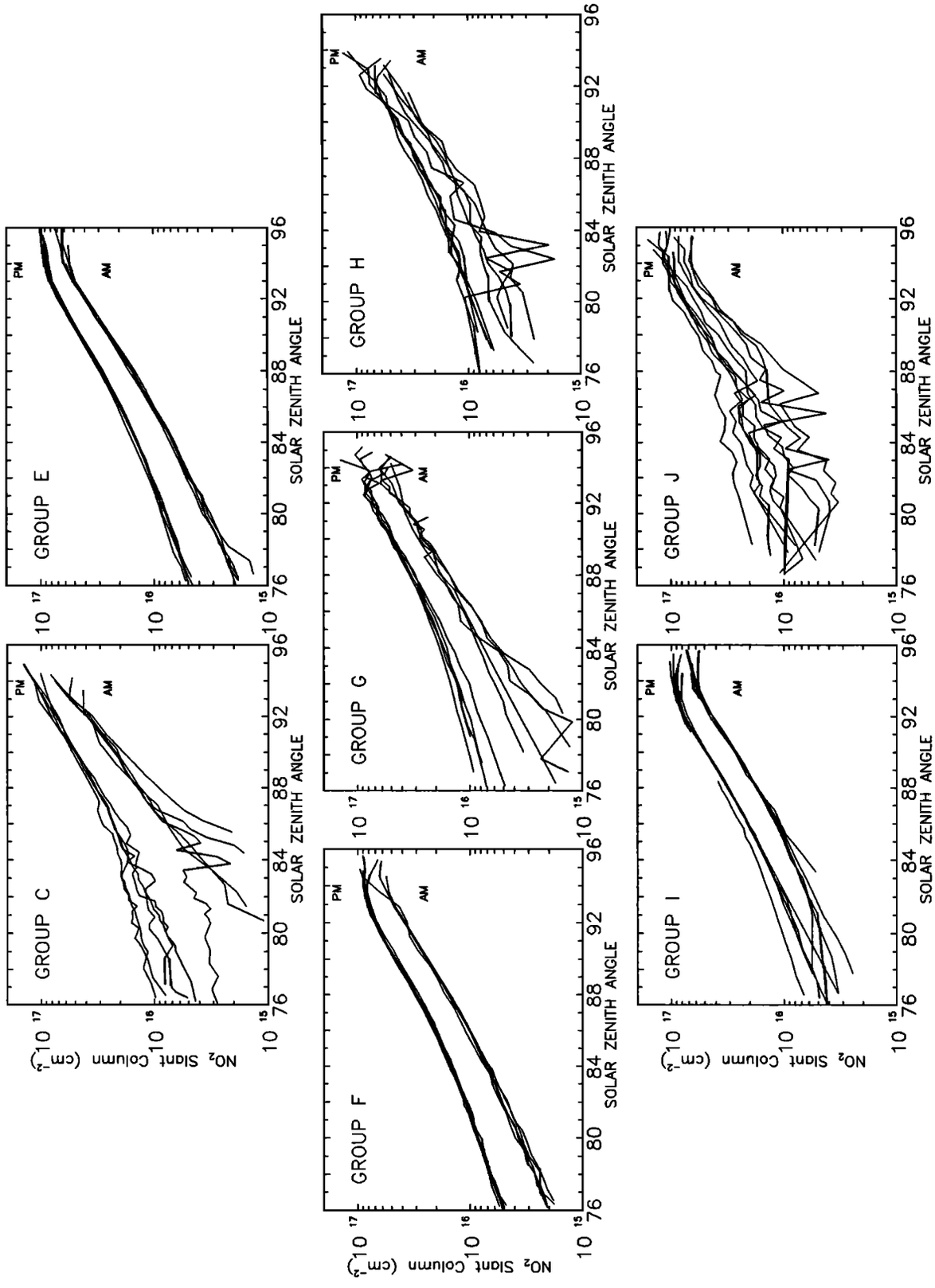


**Figure 13.** Morning and evening values of $NO_2$ slant column versus solar zenith angle measured by each group on days 134 to 138 for $I_0$ measured on each day.

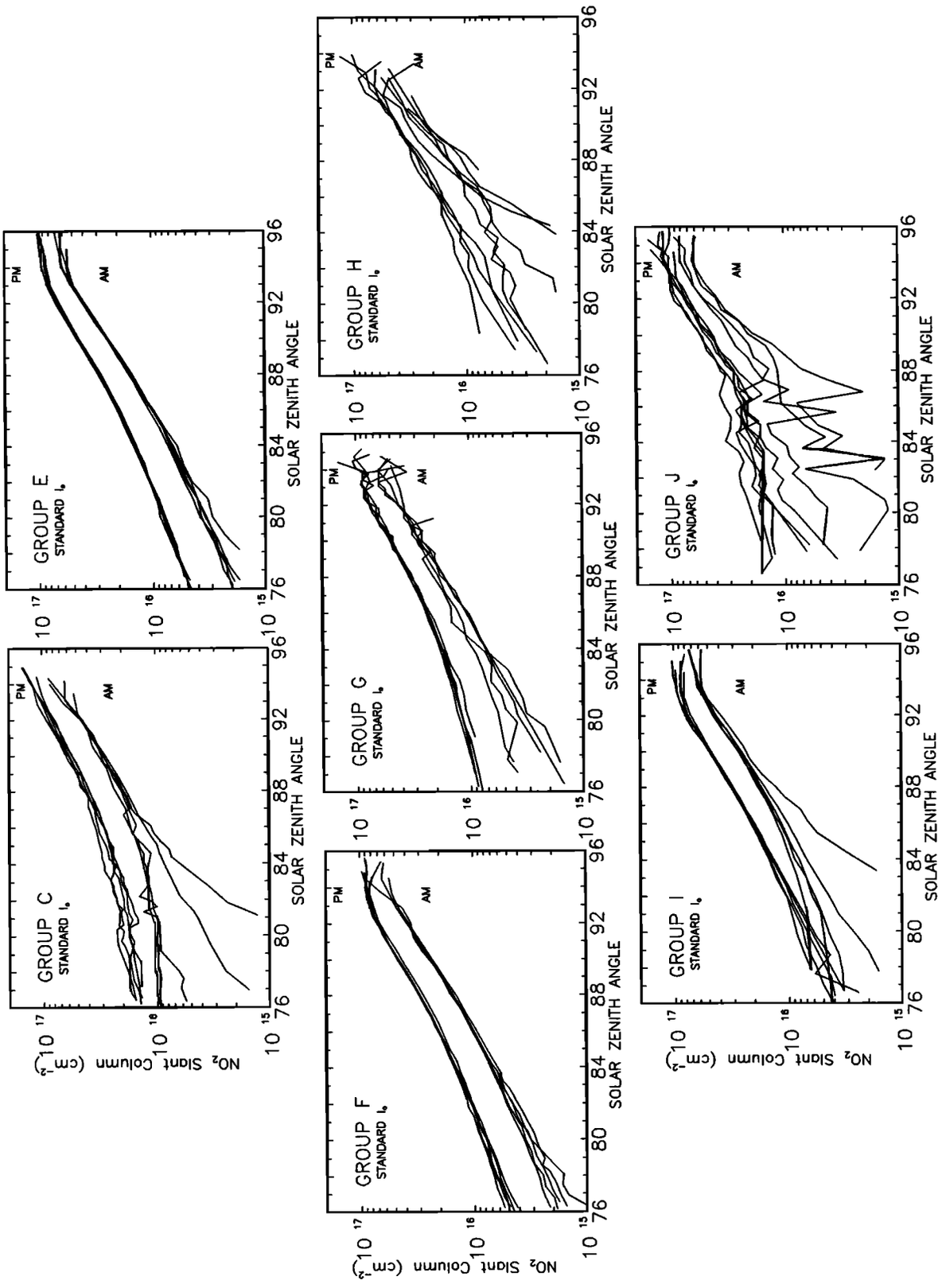


**Figure 14.** Same as Figure 13 but using a standard $I_o$.

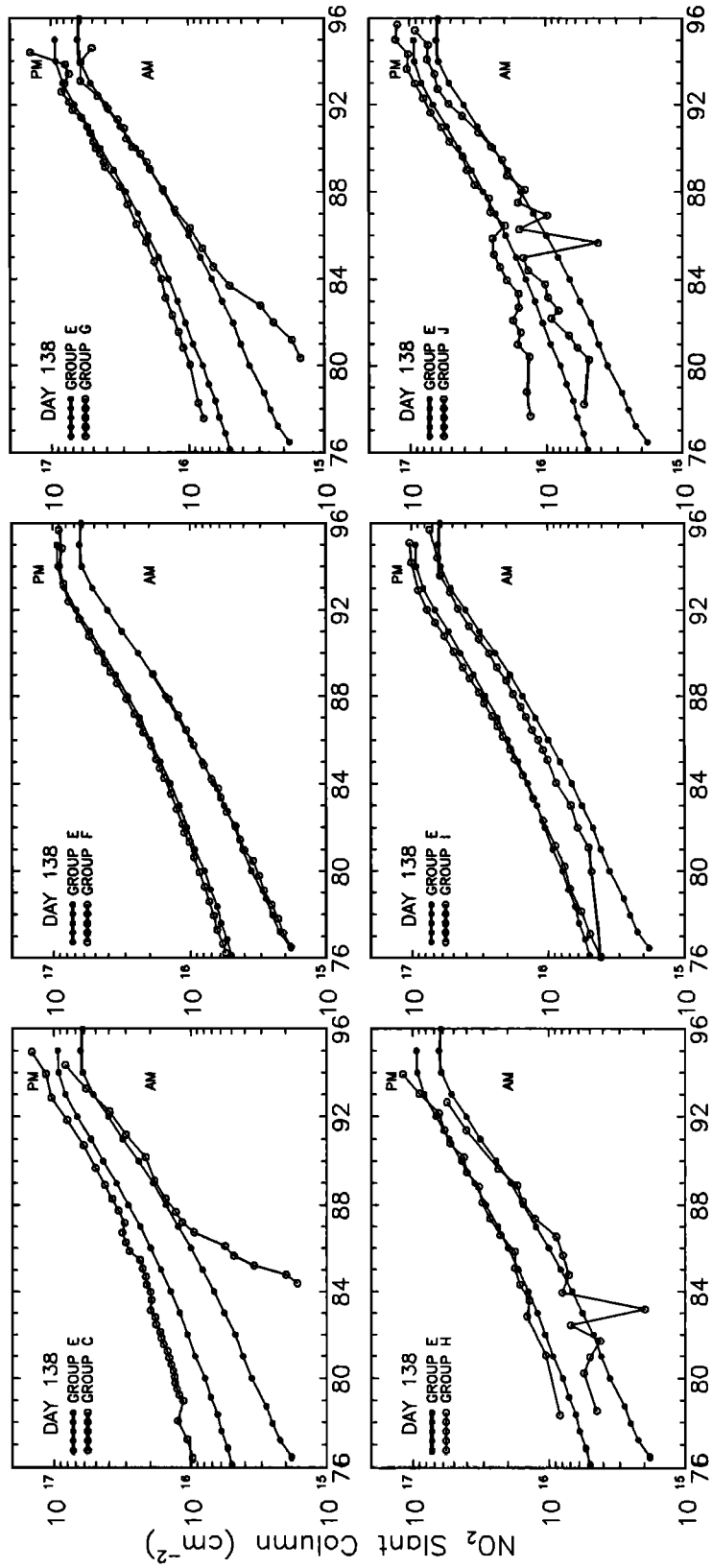


**Figure 15.** Comparisons of morning and evening values of $NO_2$ slant column versus solar zenith angle measured by six groups (open circles) with the host group E (solid circles) using daily $I_0$ on day 138.

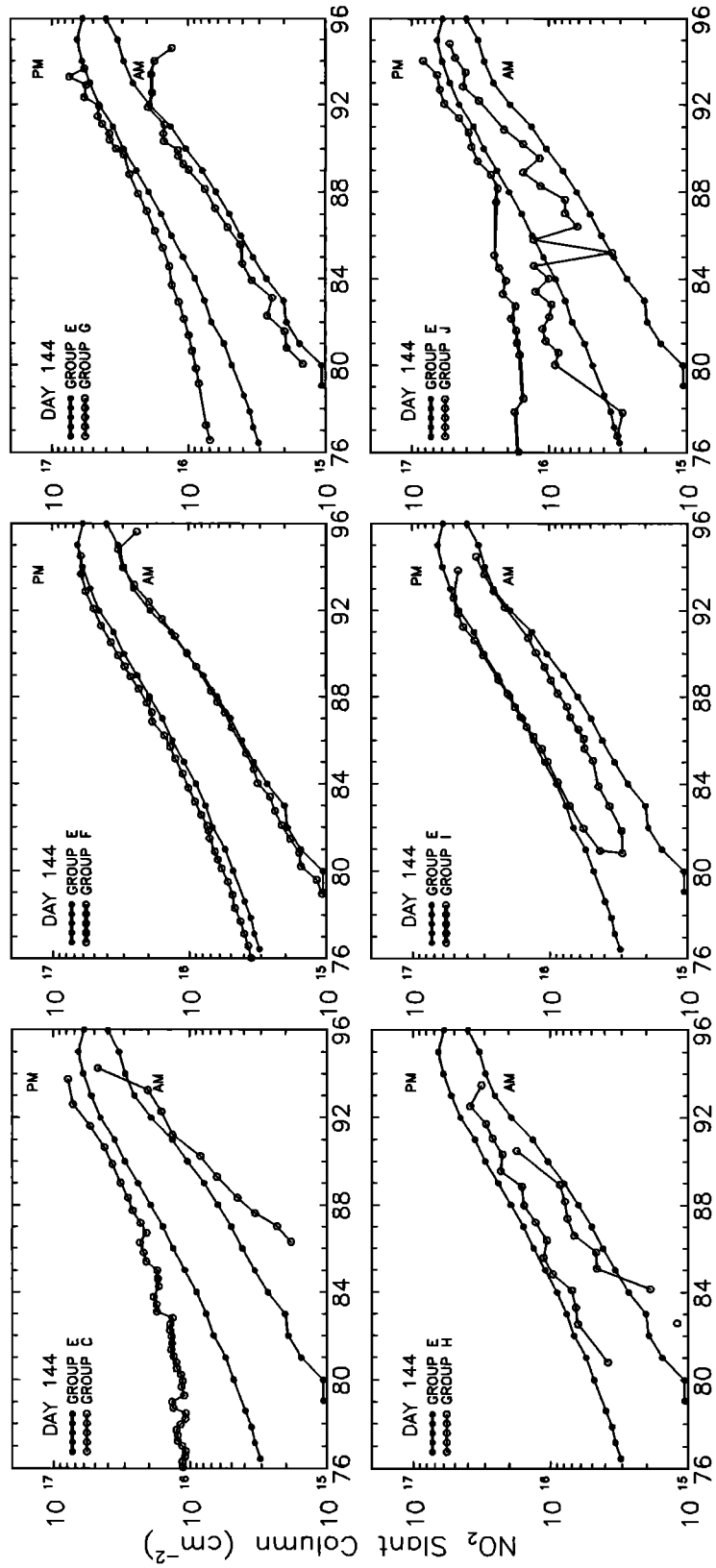


**Figure 16.** Same as Figure 15 but for day 144.

J appear to diverge from group E at small SZA in a similar fashion on both days; in particular, for the P.M. they both appear to be limited to $NO_2$ column values greater than about $10^{16}$ cm-2. Group I appears to agree well with group E in the P.M. but not in the A.M. The remaining data do not appear to display any consistent characteristics.

After the intercomparison workshop, which was held October 13-15, 1992, in Boulder, Colorado, to discuss initial results, it was decided that it would be useful for each group to provide interpolated $NO_2$ slant column values using both daily and standard $I_o$ for integer values of SZA from 76° to 94°. Figures 17 through 22 show the A.M. and P.M., daily and standard $I_o$ $NO_2$ slant column values for each group, plotted versus the host group's values for the 12 days. This form of data display allows a simple comparison and is considered the final product of this intercomparison.

As can be seen in these figures, all instruments generally agree reasonably well with the New Zealand instrument for 90° SZA slant column values (denoted by large squares and diamonds in the figures) although this is not always the case. The NOAA instrument is in excellent agreement with the NIWA instrument down to slant column values as low as 1-2 x $10^{15}$ molecules cm-2. For these weak signals, the other instruments diverge significantly from the New Zealand results. This agreement between NOAA and NIWA results does not prove that they are correct but rather that unlike any other pairs of comparisons, they consistently agree over a wide range of SZAs and $NO_2$ values.

The minimum 90° SZA slant column values experienced during the Lauder intercomparison were in the 1-2 x $10^{16}$ molecules cm-2 range during the A.M. (see Figure 12). These are relatively low values associated with lingering heterogeneous chemical effects of the Pinatubo eruption. Based on this, a minimum detectable level of 1 x $10^{16}$ molecules cm-2, with a measurement accuracy of at least ±10%, for slant column 90° SZA $NO_2$ is recommended for $NO_2$ monitoring instruments for non-Antarctic work. In Antarctica, winter denitrification associated with polar stratospheric cloud formation and preconditioning for springtime ozone hole formation can result in very low $NO_2$ levels and recommended 90° SZA slant column minimum sensitivity for Antarctic work is about 2 x $10^{15}$ molecules cm-2 for a 40% measurement under denitrified conditions in winter and spring.

## 7. Discussion

Following the intercomparison and the workshop, several groups which found their values differing substantially from the New Zealand group reevaluated their results, generally including data analysis refinements. This made considerable improvements in their results. However, in order to preserve the blind nature of the intercomparison, it was decided that any changes which resulted in improvements could be documented in this report but that the revised data should appear in a separate publication, possibly as an intercomparison with the New Zealand group. In addition, instrumental improvements were made by some groups as a result of the intercomparison. The following is a brief summary of these data reevaluations and instrumental changes.

### 7.1. New Zealand Group

The Lauder results were changed following the intercomparison because of a 436-nm interference from local fluorescent lights which was discovered in some of the high-SZA spectra. The way in which buildings at Lauder were used to accommodate different groups during the intercomparison resulted in unusually high laboratory light levels. All data were reprocessed prior to the Boulder workshop in October using a wavelength interval that excluded the interference.

An intrinsic cause of noise in spectra are intensity variations caused by the movement of clouds through the *f*/5 field of view during wavelength scanning. Lauder skies are often cloudy in May, as they were during the campaign, so higher than average noise was experienced, making the errors at small SZAs higher than normal. Some of the random deviations in Figures 13 and 14 are caused by such cloud effects. A technique to reduce such noise has been successfully used on a long-path Differential Optical Absorption Spectroscopy (DOAS) spectrometer but not to date on zenith spectrometers. The overall quality of the measurement spectra was typical of that obtained by the HR320 spectrometers used both at Lauder and at some of our global sites. However, the analysis was more detailed than usual. The improved understanding obtained from the intercomparison will be applied in future data analyses.

### 7.2. Italian Group

The data were analyzed using a linear least squares algorithm incorporating the $NO_2$ differential cross sections as measured by the same spectrometer in the sprectral range around 435.8 nm, the Rayleigh mathematical spectral function, and the shift procedure to minimize the sum of squares of the residuals (SOS). No stretch is applied for spectral $NO_2$ retrieval. Following the intercomparison workshop, the data were reevaluated including the following changes, (1) spectral interpolation via three-point quadratic function, (2) use of the cross section derived from the reciprocal of the observed spectrum to minimize the Ring effect and instrumental offset, and (3) a modified iterative procedure with variable decreasing step spectral shift to minimize SOS. In comparisons with group E data, these results show a significant improvement over those reported here for group C and will be the subject of a future publication. As a result of this reevaluation, the minimum detectable column $NO_2$ for this instrument is decidedly lower than 1 x $10^{16}$ molecules cm-2.

### 7.3. French Group

The CNRS SAOZ data were reanalyzed immediately after the campaign, with little change compared with the real-time results except for the choice of the daily $I_o$ on days 133 and 135, which were changed. More recently two improvements, which are not included in the present results, were added in the spectral analysis algorithm: (1) the use of a new set of high-resolution (0.02 nm) ozone absorption cross sections in the Chappuis bands [*Brion et al.*, 1994] at 273 and 218 K, showing no temperature dependence between 514 and 630 nm, improved the removal of the ozone features in the spectra, and (2) the introduction in the calculation of a small water vapor absorption band at 444 nm peaking at 2 x $10^{-26}$ $cm^2$ and not taken into account in the past. It was found that when not removed, the water vapor band results in an underestimation of $NO_2$, which in extreme multiple scattering conditions (e.g., fog on day 135), can be as large as 6 x $10^{15}$ molecules cm-2 of $NO_2$ (slant column). This has little consequence in the

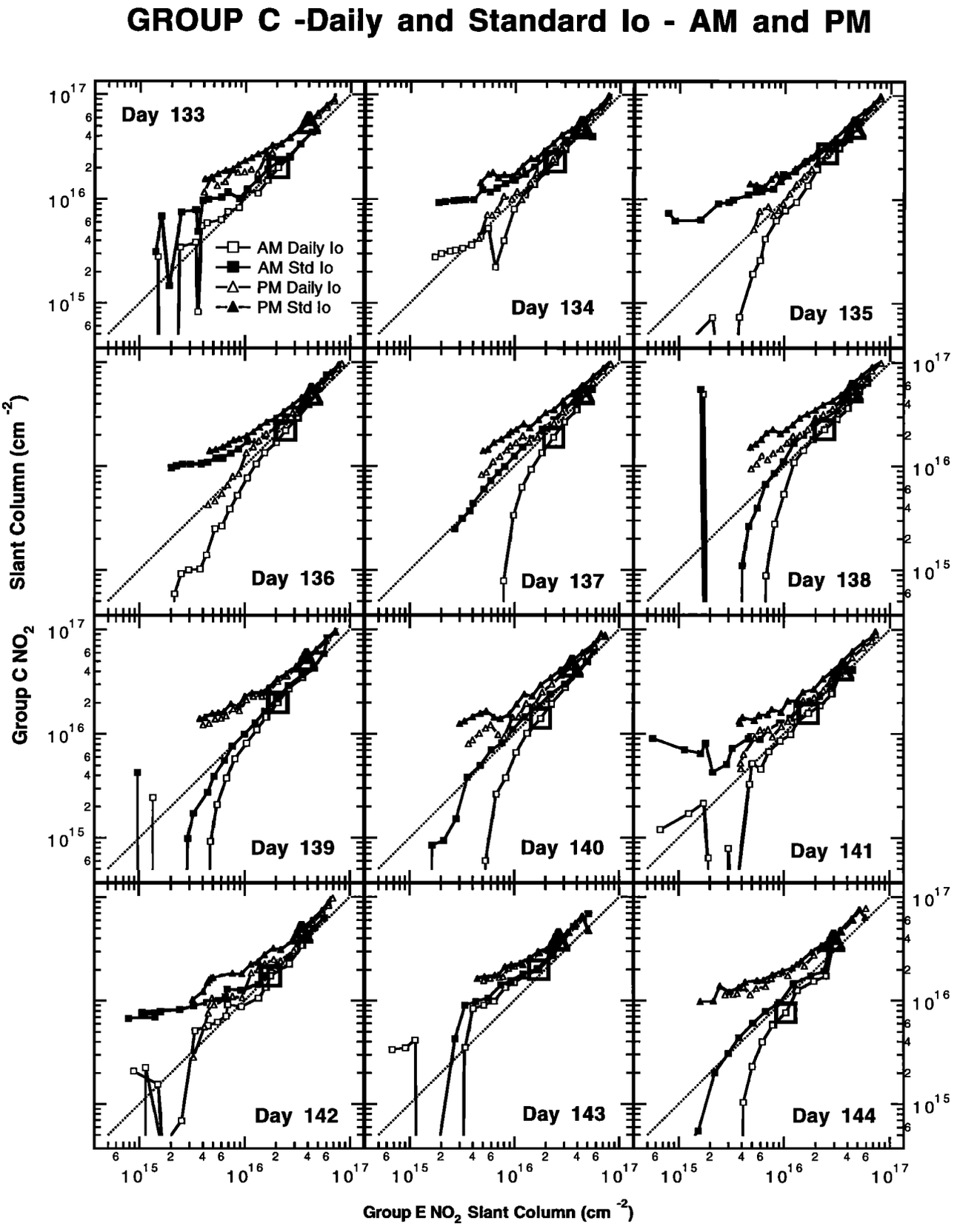


**Figure 17.** Group C morning and evening values of $NO_2$ slant column, using daily and standard $I_o$, versus the host group E values for each day of the intercomparison. The large boxes and triangles indicate the 90° solar zenith angle morning and evening values, respectively, for daily $I_o$. The dashed line represents a one to one correspondence.

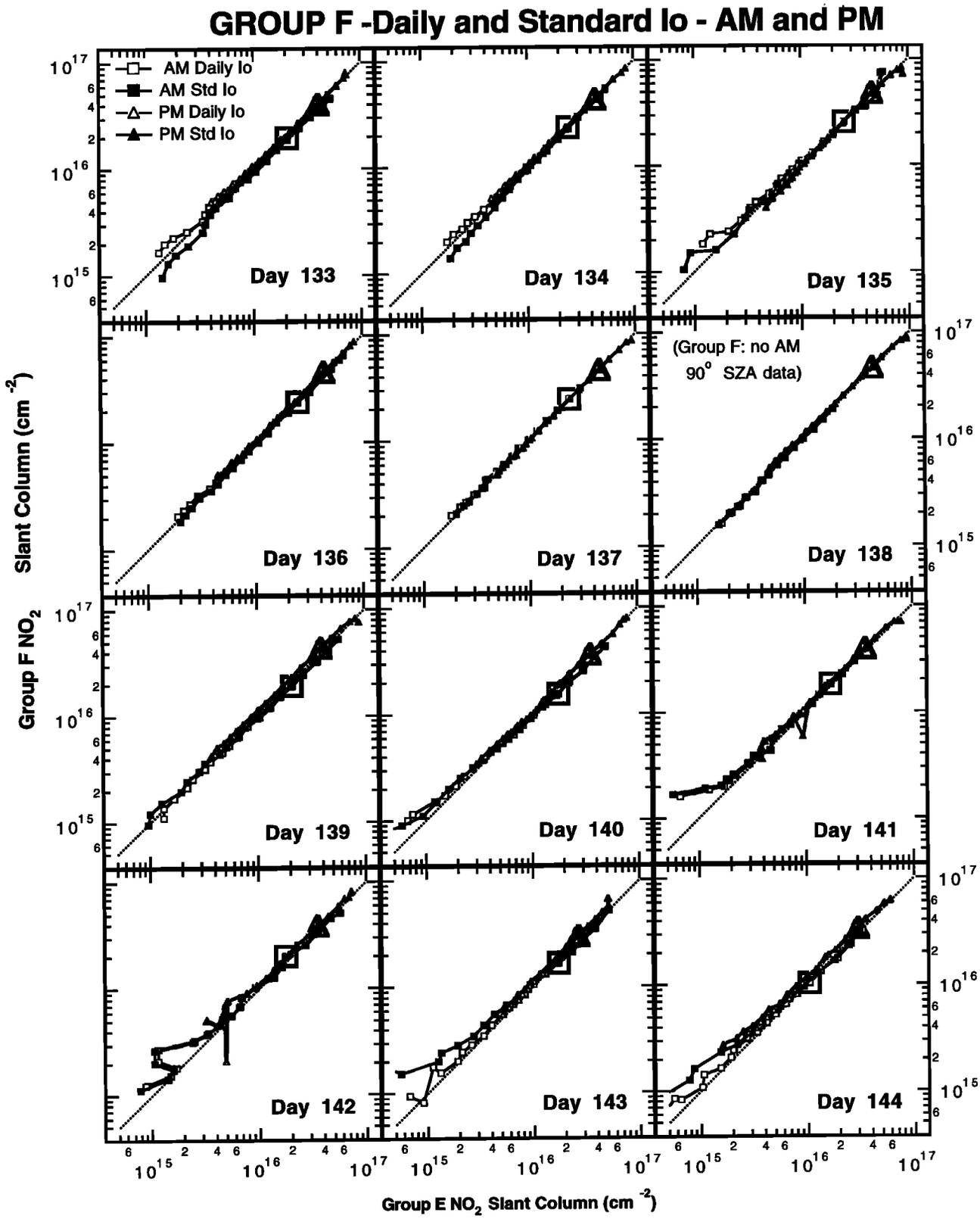


**Figure 18.** Same as Figure 17 but for group F.

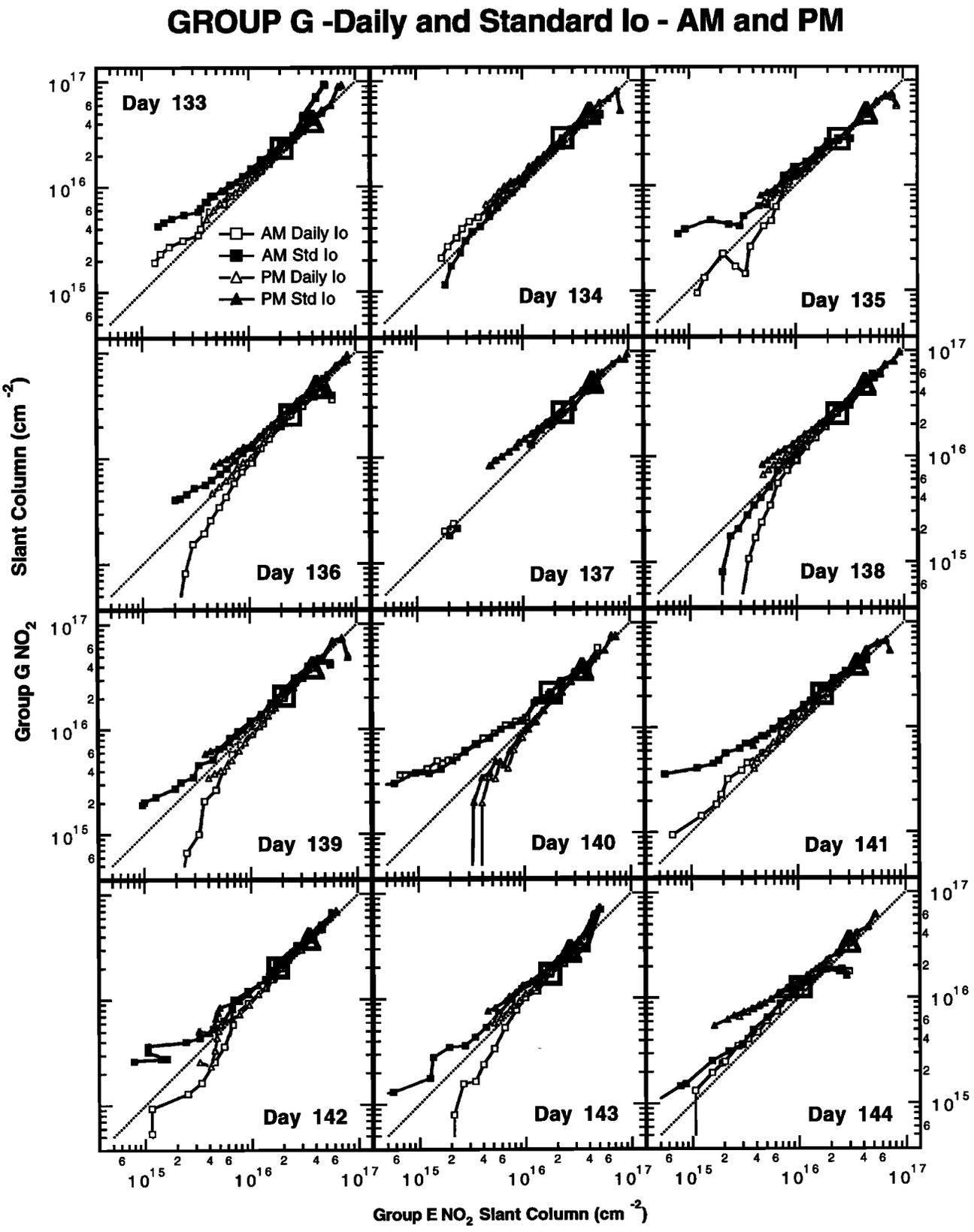


**Figure 19.** Same as Figure 17 but for group G.

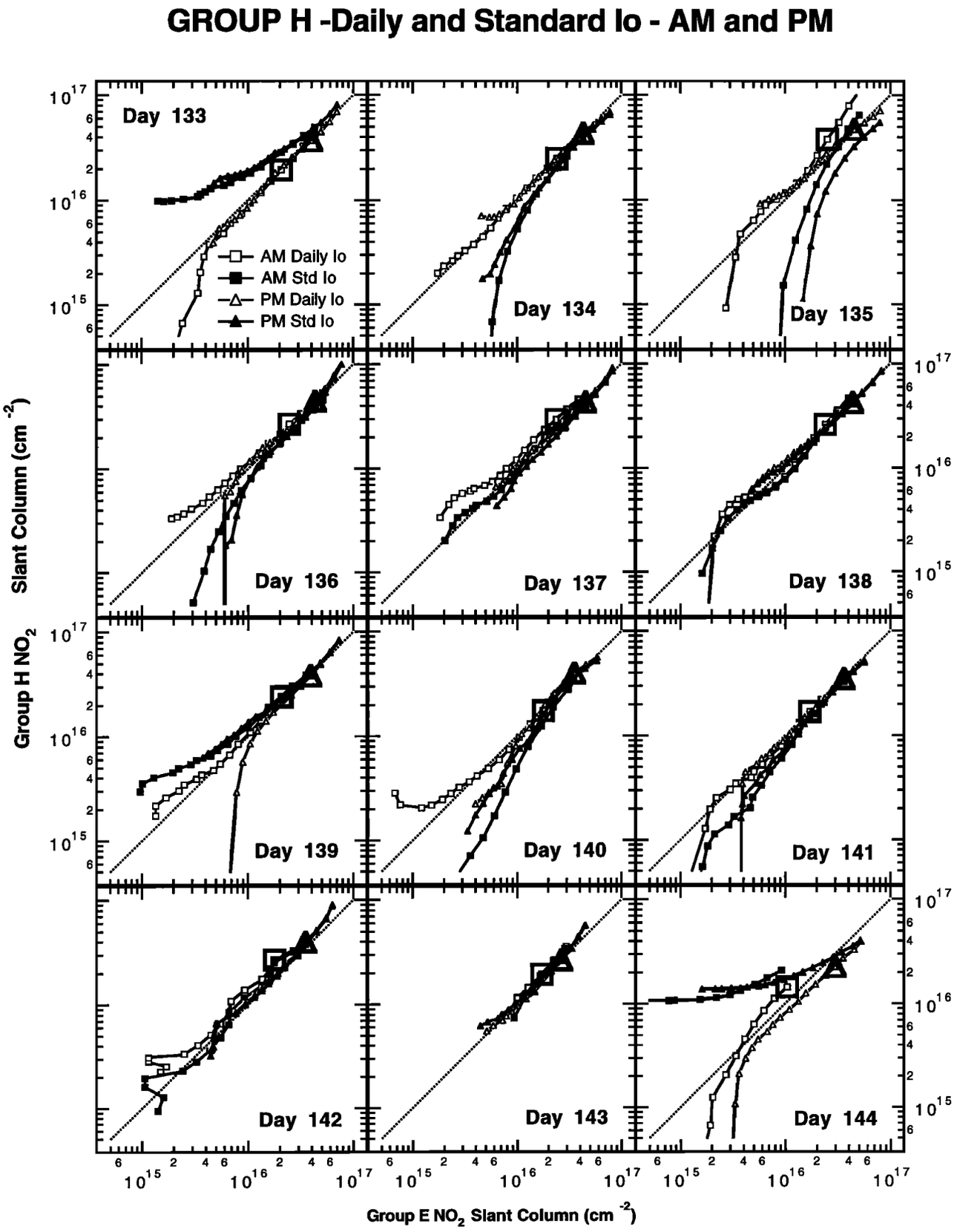


**Figure 20.** Same as Figure 17 but for group H.

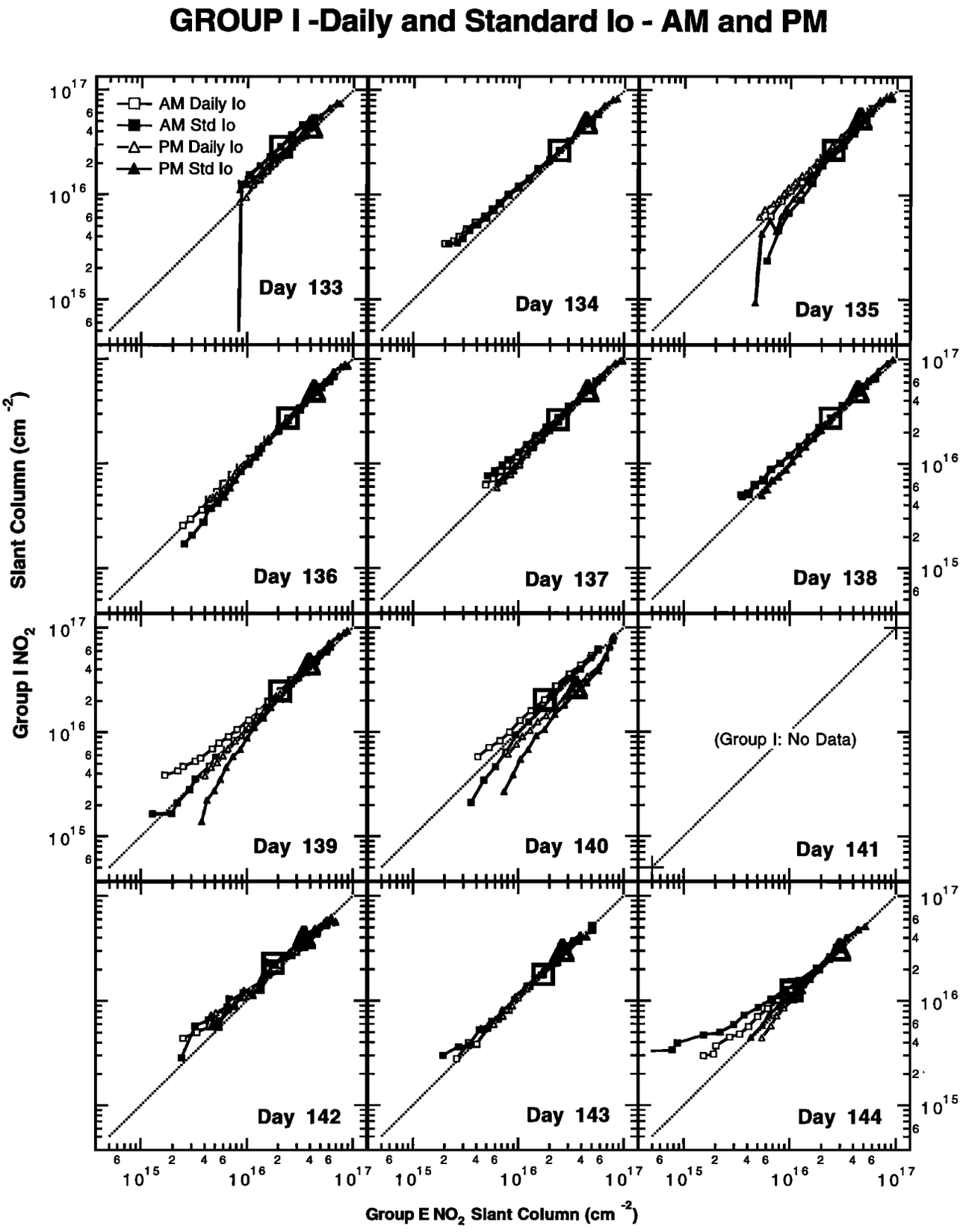


**Figure 21.** Same as Figure 17 but for group I.

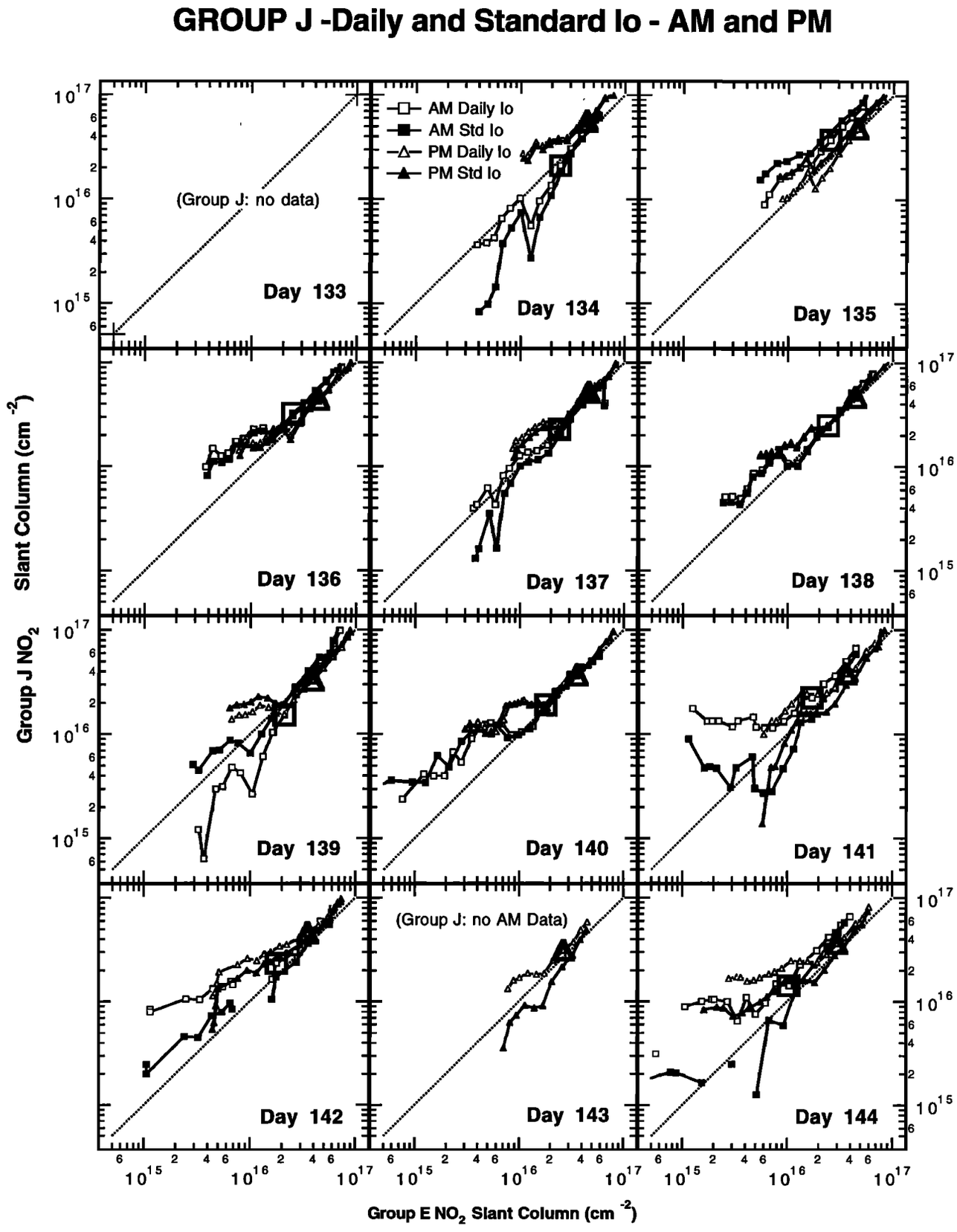


**Figure 22.** Same as Figure 17 but for group J.

measurements at twilight, but for high Sun measurements it can vary significantly from one day to another.

### 7.4. Belgian Group

Relative to the original instrument and data analysis software used to produce the data submitted for the intercomparison, a few significant changes listed below were made in order to reduce the effect of some identified deficiencies of our system.

The concept of the iterative algorithm used during the intercomparison was based on a sequence of individual determinations of the column amount of each species absorbing in the spectral region of interest using a simple linear least squares fit. Once evaluated, the contribution of each absorber was removed from the spectrum in order to progressively isolate the individual spectral signatures of all constituents. The advantage of this data analysis technique lies in the simplicity of the numerical algorithms used. However, we found that the convergence of the column amounts was difficult to obtain with good efficiency. For this reason, we opted in favor of a different analysis procedure based on a coupled linear/nonlinear least squares algorithm including shift and stretch (the latter was not included in the original iterative program) as nonlinear parameters. The application of this program to the analysis of the Lauder data resulted in significant differences for small absorptions, giving better agreement with NOAA and NIWA results at small solar zenith angles.

Following the intercomparison and according to the conclusions gathered during the workshop in Boulder, some changes were made to the instrument in order to lower its detection limit. The sampling ratio was increased from 4 to 6 diodes/FWHM by widening the entrance slit of the spectrometer in order to reduce the effect of interpolation errors in the alignment process. In addition, the control of the temperature of the spectrometer was improved, which lead to a better long-term stability of the wavelength scale. Finally, in order to enhance the differential signature of $NO_2$, the spectral resolution was increased from 1.4 to 0.8 nm FWHM by changing the grating and carefully aligning the optics of the spectrometer.

### 7.5. German Group

The etalon problems reported in section 4.5 were caused by deposition of water vapor on the cooled diode array [*Mount et al.*, 1992]. We suspect either a leak in the detector housing or an anomalous water content in the gas filling of the detector. The instrument malfunction could not be reproduced later. The spectral shift of the etalon structure during the campaign was 15 pixels in 12 days, about 15 times the typical etalon shift of our detectors of this type. The correction of the etalon by a tungsten lamp spectrum taken daily could not remove the structure; therefore other measures were taken to reduce the problem, an additional division by a fitted polynomial reduced etalon structure. Also a narrower spectral range (50 pixels from 150 pixels) was selected for the evaluation. Nevertheless, the residuals were considerably increased, leading to increased errors of the slant column. The etalon problems were even larger when the $I_o$ and the twilight spectra were taken several days apart, as was the case for the evaluation with standard $I_o$. Therefore the error of the slant column was higher for the standard $I_o$ evaluation. The results of the intercomparison campaign showed that the instrument is able to measure the $NO_2$ slant column at 90° SZA with an accuracy of 20%, even encountering the described etalon problem, which also caused the high variance of the data, especially those evaluated with the standard $I_o$.

### 7.6. U.S. Group

Two changes were made to the NOAA instrument and data analysis after it arrived back in the United States, and both were discussed at the October 1992 workshop. The changes improved the residual spectra by lowering the peak to peak noise and making them more repeatable. The first change was to include the instrument polarization as an "equivalent" molecule in the nonlinear least squares analysis. The second was to remove the detector tilt because it introduced very subtle polarization effects (the detector was tilted 4° to reflect light off the vacuum window down into a set of baffles instead of back into the light path, where it could potentially cause problems). Neither of these changes modified the $NO_2$ abundances already reported to the referee.

## 8. Summary

During the period May 12-23, 1992, seven groups from seven countries met in Lauder, New Zealand, to intercompare their remote sensing instruments for the measurement of atmospheric column $NO_2$ from the surface. The purpose of the intercomparison was to determine the degree of intercomparability and to qualify instruments for use in the Network for the Detection of Stratospheric Change. All instruments were successful in obtaining slant column $NO_2$ amounts at sunrise and sunset on most of the 12 days of the intercomparison. The group as a whole was able to make measurements of the 90° solar zenith angle slant path $NO_2$ column amount that agreed to about ±10% most of the time. However, comparisons of the individual data sets with the home (New Zealand) group, which was chosen as the basis for comparison, were not uniformly good at smaller solar zenith angles (small slant paths); i.e., the sensitivity of the measurements varied considerably. As a result of this intercomparison, some of the instruments have qualified for use in the NDSC at the lowest $NO_2$ levels. Some instruments would be incapable of measuring 90° solar zenith angle columns of $1 \times 10^{16}$ molecules $cm^{-2}$, a value somewhat larger than is present in Antarctica during the winter/spring denitrification period. Part of the sensitivity problem for these instruments is the result of instrumentation, and part is related to the data analysis algorithms used. All groups learned a great deal from the intercomparison and improved their results considerably as a result of this exercise. It is expected that these improvements, in most cases, will allow these instruments to make future measurements of $NO_2$ adequate for applications in the Network for the Detection of Stratospheric Change.

## References

Brewer, A.W., C.T. McElroy, and J.B. Kerr, Nitrogen dioxide concentrations in the atmosphere, *Nature*, *246*, 129, 1973.

Brion, J., D. Daumont, and J. Malicet, Ozone cross-sections in the Chappius bands at 273 and 218 K, Univ. de Reims, Reims, France, 1994.

Crutzen, P., The influence of nitrogen oxide on the

atmospheric ozone content, *Q. J. R. Meteorol. Soc.*, *96*, 320, 1970.

Goldman, A., Results of the UV-VIS Intercomparison-$NO_2$, $O_3$, paper presented at the UV-VIS Data Analysis Intercomparison Meeting, NDSC, Boulder, Colo., July 23-25, 1991.

Goldman, A., *UV-VIS Intercomparison II, Retrievals of $NO_2$, $O_3$, and OClO from Synthetic Spectra*, paper presented at the International $NO_2$ Instrument Intercomparison Meeting, NDSC, Boulder, Colo., Oct. 13-15, 1992.

Goutail, F., J.-P. Pommereau, and A. Sarkissian, Four years of ground-based total ozone measurements by visible spectrometry in Antarctica, in Ozone in the Troposphere and Stratosphere, Proceedings, Quadrennial Ozone Symposium, 1992, NASA Conf. Publ., *CP*-3266, 602-605, 1994a.

Goutail, F. J., J. Pommereau, A. Sarkissian, E. Kyro, and V. Dorokhov, Total nitrogen dioxide at the Arctic polar circle since 1990, *Geophys. Res. Lett.*, *21*, 1371, 1994b.

Grainger, J. and J. Ring, Anomalous Fraunhofer line profiles, *Nature*, *193*, 762, 1962.

Harrison, A.W., Midsummer stratospheric $NO_2$ at latitude 45°S, *Can. J. Phys.*, *57*, 1110, 1979.

Johnston, H., Reduction of stratospheric ozone by nitrogen oxide catalysis from SST exhaust, *Science*, *173*, 517, 1971.

Johnston, H. and J. Podolske, Interpretation of stratospheric photochemistry, *Rev. Geophys.*, *16*, 491, 1978.

Johnston, P.V., R. McKenzie, G. Keyes, and W.A. Matthews, Observations of depleted stratospheric $NO_2$ following the Pinatubo volcano eruption, *Geophys. Res. Lett.*, *19*, 211, 1992.

Jet Propulsion Laboratory (JPL), Chemical kinetics and photochemical data for use in stratospheric modeling, Evaluation # 10, *JPL Publ.*, *92-20*, 1992.

Kondo, Y., W.A. Matthews, S. Solomon, M. Koike, M. Hayashi, K. Yamazaki, N. Nakajima, and K. Tsukui, Ground-based measurements of column amounts of $NO_2$ over Syowa Station, Antarctica, *J. Geophys. Res.*, *99*, 14,535, 1994.

Kerr, J.B., Ground-based neasurements of nitrogen dioxide using the Brewer spectrophotometer, in *Ozone in the Atmosphere*, edited by R.D. Bojkov and P. Fabian, pp. 725-727, A. Deepak Publ., Hampton, VA, 1989.

Leroy, B., P. Rigaud, and E. Hicks, Visible absorption cross sections of $NO_2$ at 298 K and 235 K, *Ann. Geophys., Ser. A*, *5*, 247, 1987.

McKenzie, R.L. and P.V. Johnston, Seasonal variations in stratospheric $NO_2$ at 45°S, *Geophys. Res. Lett.*, *9*, 1255, 1982.

McKenzie, R.L. and P.V. Johnston, Stratospheric ozone observations simultaneous with $NO_2$ at 45°S, *Geophys. Res. Lett.*, *10*, 337, 1983.

McKenzie, R.L. and P.V. Johnston, Springtime $NO_2$ in Antarctica, *Geophys. Res. Lett.*, *11*, 73, 1984.

McKenzie, R.L., P.V. Johnston, C.T. McElroy, J.B. Kerr, and S. Solomon, Altitude distributions of stratospheric constituents from ground-based measurements at twilight, *J. Geophys. Res.*, *96*, 15,499, 1991.

Mount, G., R. Sanders, A. Schmeltekopf, and S. Solomon, Visible spectroscopy at McMurdo Station, Antarctica 1. Overview and daily variations of $NO_2$ and $O_3$ during austral spring 1986, *J. Geophys. Res.*, *92*, 8320, 1987.

Mount, G., R. Sanders, and J. Brault, Interference effects in reticon photodiode array detectors, *Appl. Opt.*, *31*, 851, 1992.

Noxon, J., Nitrogen dioxide in the stratosphere and troposphere measured by ground based absorption spectroscopy, *Science*, *189*, 547, 1975.

Noxon, J., Stratospheric $NO_2$. 2. Global behavior, *J. Geophys. Res.*, *84*, 5067, 1979.

Noxon, J., E. Whipple, and R. Hyde, Stratospheric $NO_2$. 1. Observational method and behavior at midlatitude, *J. Geophys. Res.*, *84*, 5047, 1979.

Perliski, L. and S. Solomon, Radiative effects of Mt. Pinatubo aerosols on ground based visible spectroscopy measurements of stratospheric $NO_2$, *Geophys. Res. Lett.*, *19*, 1923, 1992.

Perliski, L. and S. Solomon, On the evaluation of air mass factors for near-UV and visible absorption spectroscopy, *J. Geophys. Res.*, *98*, 10,363, 1993.

Perner, D., A. Roth, and T. Klupfel, Ground based measurements of stratospheric OClO, $NO_2$, and $O_3$ at Sondre Stromfjord in winter 1991/92, *Geophys. Res. Lett.*, *21*, 1367, 1994.

Pommereau, J.-P. and F. Goutail, $O_3$ and $NO_2$ ground-based measurements by visible spectrometry during Arctic winter and spring 1988, *Geophys. Res. Lett.*, *15*, 891, 1988a.

Pommereau, J.-P. and F. Goutail, Stratospheric $O_3$ and $NO_2$ observations at the southern polar circle in summer and fall 1988, *Geophys. Res. Lett.*, *15*, 895, 1988b.

Pommereau, J.-P. and J. Piquard, Ozone and nitrogen dioxide vertical distributions by UV-visible solar occultation from balloons, *Geophys. Res. Lett.*, *21*, 1227, 1994.

Ridley, B.A., S.H. Luu, D.R. Hastie, H.I. Schiff, J.C. McConnell, W.F.J. Evans, C.T. McElroy, J.B. Kerr, H. Fast, and R.S. O'Brien, Stratospheric odd nitrogen: Measurements of HNO3, NO, $NO_2$, and $O_3$ near 45°N in winter, *J. Geophys. Res.*, *89*, 4797, 1984.

Roscoe, H.K. and A.K. Hind, The equilibrium constant of $NO_2$ with $N_2O_4$ and the temperature dependence of the visible spectrum of $NO_2$: A critical review and the implications for measurements of $NO_2$ in the polar stratosphere, *J. Atmos. Chem.*, *16*, 257, 1993.

Sanders, R., S. Solomon, M. Carroll, and A. Schmeltekopf, Visible and near-UV spectroscopy at McMurdo Station, Antarctica 4. Overview and daily measurements of $NO_2$, $O_3$, and OClO during 1987, *J. Geophys. Res.*, *94*, 11,381, 1989.

Shibasaki, K., N. Iwagami, and T. Ogawa, Stratospheric nitrogen dioxide observed by ground-based and balloon-borne techniques at Syowa Station (69.0°S, 39.6°E), *Geophys. Res. Lett.*, *13*, 1268, 1986.

Solomon, S., A. Schmeltekopf, and R. Sanders, On the interpretation of zenith sky absorption measurements, *J. Geophys. Res.*, *92*, 8311, 1987.

Syed, M. and A. Harrison, Seasonal trend of stratospheric $NO_2$ over Calgary, *Can. J. Phys.*, *59*, 1278, 1981.

Wahner, A., R.O. Jakoubek, G.H. Mount, A.R. Ravishankara, and A.L. Schmeltekopf, Remote sensing observations of daytime column $NO_2$ during the Airborne Antarctic Ozone Experiment, August 22 to October 2, 1987, *J. Geophys. Res.*, *94*, 16,619, 1989.

P. Bonasoni, F. Evangelisti, and G. Giovanelli, Istituto FISBAT, CNR, Bologna, Italy.

M. DeMaziere, P. Simon, and M. Van Roozendael, Belgian Institute for Space Aeronomy, Ringlaan 3, B-1180 Brussels, Belgium.

A. Goldman, Department of Physics, University of Denver, Denver, CO 80216.

F. Goutail, J.-P. Pommereau, and A. Sarkissian, Service D'Aéronomie, CNRS, B.P. 3, 91371 Verrières le Buisson, France.

J. Harder, R. Jakoubek, G. Mount, and S. Solomon, NOAA Aeronomy Laboratory, Boulder, CO 80303.

D. Hoffman, NOAA Climate Monitoring and Diagnostics Laboratory, Boulder, CO 80303.

P. Johnston, W. A. Matthews, R. McKenzie, and A. Thomas, National Institute of Water and Atmospheric Research, Lauder, New Zealand.

J. Kerr and E. Wu, Atmospheric Environment Service, 4905 Dufferin Street, Downsview, Ontario, Canada M3H 5T4.

V. Platt and J. Stutz, Institute Für Umweltphysik, Universität Heidelberg, Heidelberg, Federal Republic of Germany.

(Received September 13, 1994; revised February 10, 1995; accepted February 11, 1995.)